Eur. Phys. J. A **8**, 307–329 (2000)

THE EUROPEAN PHYSICAL JOURNAL A

Accurate masses of unstable rare-earth isotopes by ISOLTRAP

D. Beck[1,a,b], F. Ames[2], G. Audi[3], G. Bollen[4,c], F. Herfurth[1], H.-J. Kluge[1], A. Kohl[1], M. König[1], D. Lunney[3], I. Martel[5], R.B. Moore[6], H. Raimbault-Hartmann[4], E. Schark[2], S. Schwarz[1,c], M. de Saint Simon[3], J. Szerypo[7,d], and the ISOLDE Collaboration[4]

[1] GSI, D-64291 Darmstadt, Germany
[2] Institut für Physik, Universität Mainz, D-55099 Mainz, Germany
[3] CSNSM-IN2P3-CNRS, F-91405 Orsay-Campus, France
[4] CERN, CH-1211 Geneva, Switzerland
[5] Instituto de Estructura de la Materia, CSIC, Madrid, Spain
[6] Foster Radiation Laboratory, McGill University, Montreal, H3A 2B1, Canada
[7] Institute of Experimental Physics, Warsaw-University, PL-00681 Warsaw, Poland

Received: 18 April 2000 / Revised version: 5 July 2000
Communicated by D. Schwalm

Abstract. Direct mass measurements of neutron-deficient rare-earth isotopes in the vicinity of ^{146}Gd were performed with the Penning trap mass spectrometer ISOLTRAP at ISOLDE/CERN. This paper reports on the measurement of more than 40 isotopes of the elements praseodymium, neodymium, promethium, samarium, europium, dysprosium and holmium, that have been measured with a typical accuracy of $\delta m \approx 14\,\mathrm{keV}$. An atomic mass evaluation has been performed taking into account other experimental mass values via a least-squares adjustment. The results of the adjustment are discussed.

PACS. 21.10.Dr Binding energies and masses

1 Introduction

Nuclides around the nucleus ^{146}Gd have been of considerable interest for many years. ^{146}Gd exhibits some of the features of a doubly magic nucleus due to the closure of the neutron shell at $N = 82$ and a proton sub-shell closure at $Z = 64$. The determination of the strength of such a sub-shell closure, the request for reliable and highly accurate ground-state masses ($\delta m < 20\,\mathrm{keV}$) as input data for shell model calculations [1], and the test of mass model predictions are the motivation for mass measurements in this region. Most of the masses of nuclides with $Z \leq 64$ and $N \geq 82$ are known with high precision. But this situation changes only a few neutrons and protons further away from β-stability. Prior to the ISOLTRAP measurements the experimentally determined mass values around ^{146}Gd were linked mainly by Q-values. This method often suffers from an incomplete knowledge of the decay schemes. Furthermore, since Q-values are mass differences, the error bars become quite large. This is due to adding up the uncertainties of the links in long decay chains which are required to connect an exotic nucleus to one with a known mass. Indeed, in the case of rare-earth isotopes the mass uncertainties increase drastically as one recedes far from stability and a number of previous mass determinations in this region are doubtful [2].

A completely different approach is direct mass measurement by the determination of the cyclotron frequencies of ions confined in Penning traps [3] or storage rings [4]. Common to all these experiments is the determination of the angular cyclotron frequency

$$\omega_\mathrm{c} = \frac{q}{m} \cdot B \tag{1}$$

of ions with a charge-to-mass ratio q/m confined in a magnetic field B. The value of the magnetic field B required for the mass determination can be determined from the cyclotron frequency ω_c of an ion with a well-known mass.

Penning traps presently provide the highest accuracy, reaching $\delta m/m \approx 10^{-10}$ in the case of light, stable nuclei [5,6]. They can be advantageously applied to short-lived radioactive ions, as demonstrated by the tandem Penning trap spectrometer ISOLTRAP [7] installed at ISOLDE/CERN [8,9]. ISOLTRAP has been designed particularly for mass measurements of unstable nuclides. Masses of more than 100 nuclei, most of them far from stability, and some with half-lives down to one second, have

[a] e-mail: `dietrich.beck@fys.kuleuven.ac.be`
[b] *Present address*: Instituut voor Kern- en Stralingsfysica, K.U. Leuven, Celestijnenlaan 200 D, B-3001 Leuven, Belgium
[c] *Present address*: NSCL, Michigan State University, East Lansing, MI-48824, USA
[d] *Present address:* Department of Physics, University of Jyväskylä, PB 35 (Y5), FIN-40351 Jyväskylä, Finland

been determined with an accuracy of about $1 \cdot 10^{-7}$ and a resolving power of typically one million [10–13,26]. Prior to the measurements reported here the applicability was restricted to isotopes of alkali and alkali-earth elements. Measurements of rare-earth isotopes were impossible due to large isobaric contamination of these ISOLDE beams. This was overcome after the installation of a special cooler Penning trap which acts as an isobar separator [14].

This paper reports on mass measurements of 44 rare-earth isotopes and of ^{123}Ba, ^{125}Ba, ^{127}Ba and ^{131}Ba produced by 1 GeV-proton–induced spallation of a tantalum target. The nuclides were ionized in a tungsten surface ionization source. After a first separation step by the ISOLDE mass separator the ions were transported to the experiment with an energy of 60 keV. The masses of the nuclides in this work have been measured to a great part also by Schottky mass spectrometry at the experimental storage ring ESR at GSI [15]. In general, good agreement between ISOLTRAP and ESR data is observed, and the Penning trap data have usually an accuracy of almost an order of magnitude better than the Schottky data.

This paper is structured as follows. Section 2 describes those features of the ISOLTRAP experiment which are relevant for this work. The measurements and the experimental results are presented in section 3. Section 4 describes an atomic mass evaluation, where the experimental results of this work are combined with all known experimental data on atomic masses. The outcome of this mass evaluation is then discussed in section 5. Due to the amount of data presented the main text was kept short. Additional information is included in the appendix.

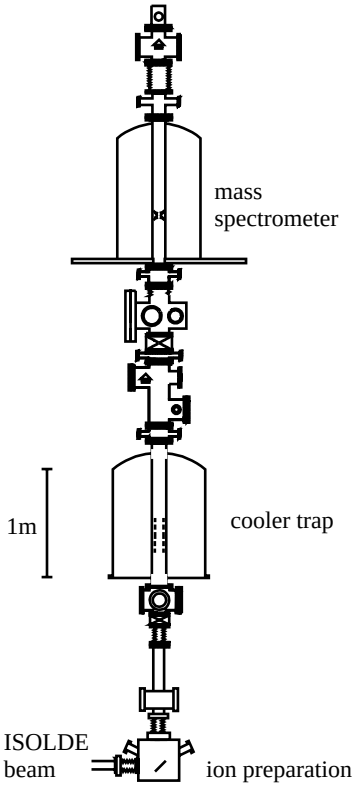

Fig. 1. The ISOLTRAP spectrometer installed at ISOLDE/CERN. The lower trap acts as an ion beam buncher, cooler and isobar separator. The upper trap is operated as a high-accuracy mass spectrometer.

2 The ISOLTRAP experiment

2.1 Experimental setup

Figure 1 shows the experimental setup of ISOLTRAP [7] installed on the central beam line of the on-line mass separator ISOLDE at CERN. The essential parts of the spectrometer are an ion beam preparation section and two Penning traps. The first Penning trap serves for accumulation, purification and cooling of the ions as well as for the production of ion bunches suitable for transfer to the second trap. The second trap is a high-precision trap for the determination of the cyclotron frequency.

For the preparation of a low-energy ion beam suitable for transfer into the first Penning trap, the 60 keV continuous ISOLDE beam is first collected on a foil of a secondary ion source system[1]. Low-energy ions are produced via surface ionization by heating the foil.

The first trap is a large cylindrical Penning trap placed in the homogeneous field of a 4.7 T superconducting magnet. The continuous low-energy ion beam delivered from the ion preparation system is captured in the trap and mass selectively cooled by interaction with buffer gas and an azimuthal radio-frequency (rf) field. Only when this frequency equals the cyclotron frequency of the nuclide under investigation, is this cooled into the center of the trap. The ions can then be extracted through a diaphragm and transferred to the second trap. A detailed description of the cooler trap and the cooling technique can be found in [14] and [17].

In the second trap, which is a precision Penning trap used as a mass spectrometer, the ion motion is driven by an azimuthal rf-field of frequency ω_{rf}. If $\omega_{\mathrm{rf}} = \omega_{\mathrm{c}} = (q/m) \cdot B$, an increase of the amplitude of the cyclotron motion of the stored ions is achieved [18]. This change in the ion motion is accompanied by an increase of energy in the radial plane as well as of the magnetic moment of the ion orbit. The increase of energy in resonance is detected by a time-of-flight technique. After excitation, the ions are ejected from the trap and allowed to drift through the inhomogeneous fringe field of the magnet to an ion detector. The inhomogeneous magnetic field gives rise to an axial force due to the orbital magnetic moment. Therefore, ions in resonance with the rf-field, *i.e.* those excited at the cyclotron frequency, reach the detector faster than those off resonance. Hence, the determination of the time-of-flight as a function of the frequency ν_{rf} of the rf-field leads to a resonance, as shown in fig. 2 for the example of ^{134}Nd. The solid line is the theoretically expected line shape [18] of such a resonance adjusted to fit the data points.

[1] Recently, this ion source has been replaced by a linear radio-frequency quadrupole ion beam buncher [16].

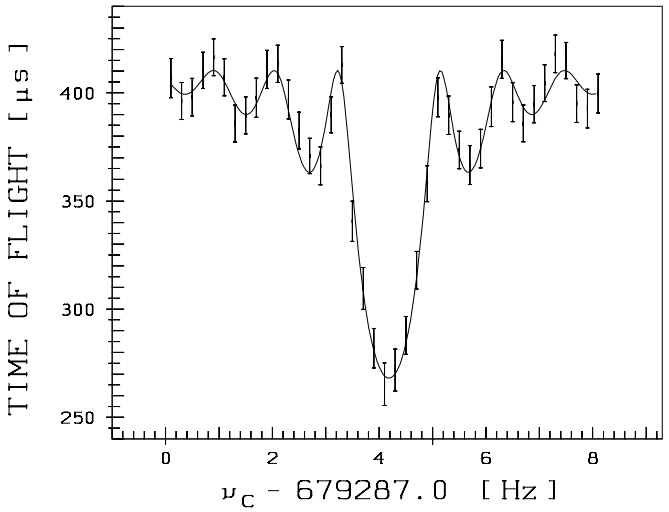

Fig. 2. Cyclotron resonance curve for ^{134}Nd. Shown is the time of flight of the ions from the trap to an ion detector as a function of the applied radio frequency. The solid line is a fit of the theoretical line shape to the data points.

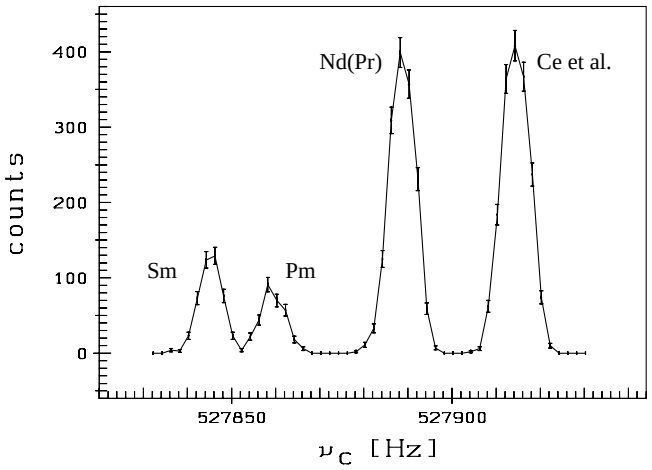

Fig. 3. Mass scan with the cooler trap of an $A = 138$ beam delivered by ISOLDE. Shown is the number of ejected ions as a function of the applied radio frequency.

The resonance width $\Delta\nu_{\mathrm{FWHM}}$ determines the resolving power $R = \nu_{\mathrm{c}}/\Delta\nu_{\mathrm{FWHM}}$ of the spectrometer. This width is approximately equal to the inverse of the period T_{rf} during which the ions experience the rf-field inside the trap. As an example, for ions with $A \approx 85$ the cyclotron frequency is $\nu_{\mathrm{c}} \approx 1\,\mathrm{MHz}$ in a magnetic field of $B = 6\,\mathrm{T}$. Using $T_{\mathrm{rf}} = 12\,\mathrm{s}$, resolving powers of $R \approx 1 \cdot 10^7$ have been achieved with ISOLTRAP [19]. For optimum use of beam time the ISOLTRAP spectrometer is usually operated with a resolving power of about $R \approx 10^6$ ($T_{\mathrm{rf}} = 0.9\,\mathrm{s}$), which allows mass determination within an accuracy of $\delta m/m \approx 1 \cdot 10^{-7}$ [10–13,26].

2.2 Treatment of contaminated beams

Test measurements and analysis of the data showed that, except for magnetic field variations, the only relative frequency shift that in some cases exceeds $\delta\nu/\nu \approx 1 \cdot 10^{-7}$ is due to contamination of the investigated nuclide by another species with a different mass [10] (see section 3.2.1). Since the radioactive nuclides are selected by the ISOLDE mass separator according to their mass number, only isobars and isomers have to be considered as possible contamination.

The effect of such contamination has been discussed in detail in [10,21]. One has to distinguish two situations, one in which the mass resolution of the spectrometer is sufficient to resolve the different species and the other in which this is not the case. In most of the reported measurements the spectrometer was operated with a resolving power of $R \approx 650000$ ($T_{\mathrm{rf}} = 0.9\,\mathrm{s}$) which corresponds to a mass difference of $\Delta m(\mathrm{FWHM}) \approx 200\,\mathrm{keV}$. In general the effects due to contamination are roughly proportional to the number of the contaminating ions and can be reduced by storing only a few ions simultaneously [10]. A contamination with a mass difference larger than the corresponding line width can easily be detected by plotting the measured cyclotron frequency as a function of the number of the stored ions [10].

2.3 Obtaining isobarically pure samples

The cooler Penning trap system has been optimized for a high mass selectivity in order to resolve isobars and to deliver clean ion bunches to the precision trap, which is essential for highly accurate mass measurements [14]. The resolving power of this trap is typically $m/\Delta m(\mathrm{FWHM}) \approx 1 \cdot 10^5$. As an example, fig. 3 shows a mass scan performed with the cooler trap for an $A = 138$ ion beam delivered by ISOLDE. The isobars ^{138}Sm and ^{138}Pm separated by some 3.5 MeV are clearly resolved. By experiment it was determined that the cooler trap can accept and purify at least 100 times as many contaminating ions as those of interest, even for close lying isobars. This capability is essential for direct mass measurements on rare-earth isotopes where such levels of contamination are often encountered.

In the case of isobars the purification via the mass selective cooling procedure in the cooler trap is almost complete as shown in fig. 3, but in some cases a residual contamination might still be present. Such a contamination can be removed in the precision trap by exciting the unwanted species at its reduced cyclotron frequency. This leads to an increase of the ion's cyclotron orbit, thereby removing the contaminating species from the trap center.

2.4 Resolving isomers

The mass region around ^{146}Gd is also rich in nuclides with long-lived isomers at excitation energies less than 1 MeV. These isomers are produced together with ground state nuclei in the ISOLDE targets. The high resolving power of the precision trap, up to $m/\Delta m \approx 1 \cdot 10^7$, is usually sufficient to separate the isomeric and ground states of

Table 1. Overview of the target materials used, the nuclides investigated and the reference nuclides used for magnetic field calibration. In all cases a surface ionization source with tungsten ionizer has been used at the ISOLDE mass separator.

Run	Target	Investigated nuclide	Reference
#1	–	^{151}Eu, ^{153}Eu	^{85}Rb
#2	–	^{133}Cs	^{85}Rb
#3	Nb/Ta	^{139,140,142,143}Sm, ^{143}Eu, ^{143}Pm, ^{154}Dy	^{133}Cs
#4	Ta	$^{134,136-138}$Nd, $^{136-138}$Pm $^{136-139,142}$Sm, ^{148}Dy, ^{150}Ho	^{133}Cs
#5	Ta	^{123,125,127,131}Ba, $^{133-137}$Pr, ^{130,132,134,135,138}Nd, $^{139-141,143}$Pm, ^{137,138,141}Sm, $^{139,141-149}$Eu, ^{148,149}Dy	^{133}Cs

unstable nuclei. For many nuclei the relative production of isomeric and ground states is uncertain, and in some cases it is even not known which of the two states is the isomeric or the ground state. For an accurate ground-state mass determination it is therefore essential to be able to distinguish both states.

For ^{141}Sm the nuclei are produced both in the isomeric state ($T_{1/2} = 22.6\,\mathrm{min}$), with a known excitation energy of only 175.8(0.3) keV [22], and in the ground state ($T_{1/2} = 10.2\,\mathrm{min}$). Since the ratio of both states in the ISOLDE beam is unknown, separation of isomeric and ground states is imperative. However, the resolving power of $R \approx 650000$, as achieved with the usual excitation time of $T_{\mathrm{rf}} = 900\,\mathrm{ms}$, is not sufficient. Therefore the resolving power of the spectrometer was increased to $R \approx 3 \cdot 10^6$ by choosing $T_{\mathrm{rf}} = 4\,\mathrm{s}$. Figure 4 shows the measured cyclotron resonance curve for ^{141}Sm, where the isomeric and ground states are clearly resolved.

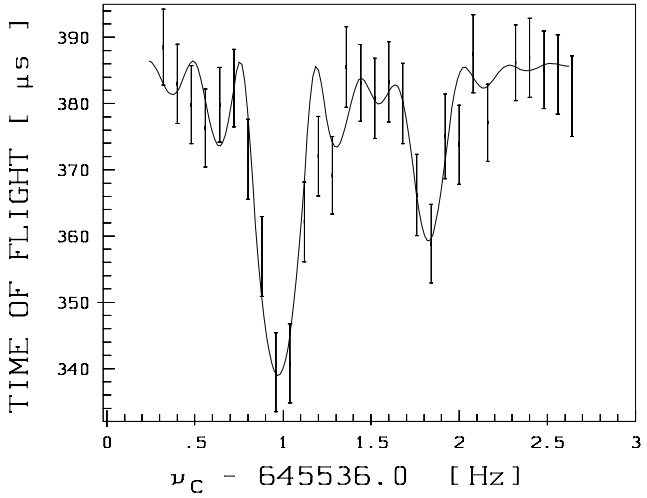

Fig. 4. Cyclotron resonances of ^{141}Sm ions in the isomeric (left) and ground state (right). Both species were stored simultaneously in the trap. From the center frequencies of the resonance curve the excitation energy of the isomer can be determined with $\Delta E = 171(4)\,\mathrm{keV}$. The solid line is a fit of the theoretical line shape to the data points.

3 Measurements and analysis

3.1 Measurements

The data presented in this work have been obtained in five on-line runs. Table 1 gives an overview of the target and ion source systems used at the ISOLDE mass separator for the production of the nuclides. The nuclides investigated and the reference nuclides, which are necessary for the calibration of the magnetic field of the precision trap, are also listed. In all cases the reference nuclide was produced with an internal ion source of the ISOLTRAP spectrometer.

During run #1 and #2 test measurements were performed with stable cesium and europium isotopes. A small amount of CsCl or EuCl was put into the ionizer of the ISOLDE target ion-source system. Thus, these measurements present a test of the spectrometer under on-line conditions.

Run #3 was the first beam time where radioactive isotopes of rare-earth were investigated. ISOLDE target #063 was used, where the target material consisted of tantalum and niobium foils in equal amount. For technical reasons the target could only be operated at a relatively low temperature of $\approx 1900\,^{\circ}\mathrm{C}$, resulting in long delay times in the target. As a consequence, only long-lived nuclides were delivered by the ISOLDE mass separator.

In run #4 target #051 was used which consisted of tantalum foils only. In order to keep the delay times for the diffusion of the nuclides short, the target was heated to $2200\,^{\circ}\mathrm{C}$ enabling us to investigate nuclides with shorter half-lives and less volatile elements.

Tantalum foil target #096 was used in run #5. The mass measurements with the ISOLTRAP spectrometer were accompanied by measurements of characteristic γ-radiation with a Ge-detector mounted at a nuclear spectroscopy tape station. This was done to obtain additional information for the identification of the delivered nuclides. This was especially important for those nuclides for which no attempt was made to resolve isomeric and ground states. Furthermore, the γ-measurements allowed to determine the ISOLDE beam intensities for a number of the investigated nuclides. Although these beam intensities can also be regarded as an experimental result, they are not in the main theme of this paper and are presented in appendix A.

During this beam time strong molecular sidebands of fluorine were observed due to a contamination of the tar-

Table 2. Frequency ratios of the nuclides investigated. The nuclides and the half-lives are listed in columns 1 and 2. Half-lives estimated from systematic trends only [22] are marked by "#". The nuclides marked by u, v, w, x, y, z are special cases which are discussed in more detail. Listed in columns 3 and 4 is the run in which the individual nuclide has been investigated, and the reference nuclide used. The frequency ratios with their statistical (first bracket) and their total error (second bracket) are given in column 5. If a nuclide has been investigated in more than one beam time, it is marked by "Average" in column 3 and the mean value is given in column 5 (see text).

Nuclide	$T_{1/2}$ (from [22])	Run	Reference	Frequency ratio ν_{ref}/ν $(\sigma_{\mathrm{stat}})(\sigma_{\mathrm{total}})$
^{133}Cs	stable	#2	^{85}Rb	1.565221527 (22)(158)
^{123}Ba	2.7 min	#5	^{133}Cs	0.924858523 (36)(99)
^{125}Ba	3.5 min	#5	^{133}Cs	0.939874523 (27)(98)
^{127}Ba	12.7 min	#5	^{133}Cs	0.954897403 (20)(98)
^{131}Ba	11.5 d	#5	^{133}Cs	0.984962860 (40)(106)
^{133}Pr	6.5 min	#5	^{133}Cs	1.000081839 (57)(115)
^{134}Pr	17 min	#5	^{133}Cs	1.007601468 (65)(120)
^{135}Pr	24 min	#5	^{133}Cs	1.015106005 (35)(107)
^{136}Pr	13.1 min	#5	^{133}Cs	1.022627033 (50)(114)
^{137}Pr	1.28 h	#5	^{133}Cs	1.030136276 (45)(113)
^{130}Nd^{19}F^{v}	28 s	#5	^{133}Cs	1.120549023 (969)(975)
^{132}Nd	1.75 min	#5	^{133}Cs	0.992610528 (375)(388)
^{134}Nd	8.5 min	average	^{133}Cs	1.007624579 (17)(102)
^{135}Nd^{z}		#5	^{133}Cs	1.015144366 (36)(108)
^{135g}Nd	12.4 min			
^{135m}Nd	5.5 min			
^{136}Nd	50.7 min	#4	^{133}Cs	1.022644223 (26)(106)
^{137}Nd	38.5 min	#4	^{133}Cs	1.030165259 (21)(105)
^{138}Nd	5.04 h	average	^{133}Cs	1.037669795 (23)(106)
^{136}Pm^{x}		#4	^{133}Cs	1.022709880 (111)(151)
^{136g}Pm	47 s			
^{136m}Pm	107 s			
^{137}Pm	2 min#	#4	^{133}Cs	1.030209781 (30)(107)
^{138}Pm	3.24 min	#4	^{133}Cs	1.037727185 (22)(106)
^{139}Pm	4.15 min	#5	^{133}Cs	1.045230454 (42)(113)
^{140m}Pm	5.95 min	#5	^{133}Cs	1.052752405 (53)(118)
^{141}Pm	20.9 min	#5	^{133}Cs	1.060254384 (37)(112)
^{143}Pm	265 d	average	^{133}Cs	1.075282971 (29)(111)
^{136}Sm	47 s	#4	^{133}Cs	1.022744338 (45)(112)
^{137}Sm^{y}		average	^{133}Cs	1.030259307 (25)(106)
^{137g}Sm	45 s			
^{137m}Sm	20 s#			

get material with stable fluorine. As an example, all investigated barium isotopes were delivered as BaF. However, the BaF molecules were dissociated in the secondary ion source of ISOLTRAP and the cyclotron frequency of pure barium ions was measured.

3.2 Cyclotron frequency ratios and data analysis

3.2.1 Obtaining a frequency ratio and its uncertainty

A cyclotron frequency is obtained by fitting the theoretically expected line shape [18] to the measured resonance curve. The magnetic field has to be known to convert the measured cyclotron frequency into a mass value. This is done by frequently measuring the cyclotron frequency of a reference nuclide before, during and after an on-line run. Typically a stable nucleus in the backbone of well-known masses is chosen as the reference nuclide. It is planned to use the atomic mass standard, *i.e.* clusters consisting of ^{12}C atoms, as reference at ISOLTRAP. For the moment, not a mass value is given as the experimental result but the ratio of the cyclotron frequencies of the nuclide investigated and the reference nuclide. A frequency ratio can be converted into an atomic mass value m by multiplica-

Table 2. (*Continued.*)

Nuclide	$T_{1/2}$ (from [22])	Run Time	Reference	Frequency Ratio ν_{ref}/ν $(\sigma_{\mathrm{stat}})(\sigma_{\mathrm{total}})$
^{138}Sm	3.1 min	average	^{133}Cs	1.037754773 (19)(106)
^{139}Sm	2.57 min	average	^{133}Cs	1.045271819 (18)(106)
^{140}Sm	14.8 min	#3	^{133}Cs	1.052771162 (43)(114)
^{141g}Sm	10.2 min	#5	^{133}Cs	1.060291390 (25)(109)
^{141m}Sm	22.6 min	#5	^{133}Cs	1.060292772 (19)(108)
^{142}Sm	72.5 min	average	^{133}Cs	1.067790904 (16)(108)
^{143}Sm	8.83 min	#3	^{133}Cs	1.075310819 (37)(114)
^{139}Eu	17.9 s	#5	^{133}Cs	1.045328216 (54)(117)
^{141}Eu	40.0 s	#5	^{133}Cs	1.060340071 (30)(110)
^{142m}Eu	1.22 min	#5	^{133}Cs	1.067856636 (27)(110)
^{143}Eu	2.63 min	average	^{133}Cs	1.075353544 (14)(108)
^{144}Eu	10.2 s	#5	^{133}Cs	1.082866586 (70)(129)
^{145}Eu	5.93 d	#5	^{133}Cs	1.090371599 (63)(126)
^{146}Eu	4.59 d	#5	^{133}Cs	1.097902808 (39)(117)
^{147}Eu	24.1 d	#5	^{133}Cs	1.105423406 (53)(122)
^{148}Eu	54.5 d	#5	^{133}Cs	1.112957695 (34)(116)
^{149}Eu	93.1 d	#5	^{133}Cs	1.120480908 (58)(126)
^{151}Eu	stable	#1	^{85}Rb	1.777377267 (21)(179)
^{153}Eu	stable	#1	^{85}Rb	1.800947577 (52)(187)
^{148}Dy	3.1 min	average	^{133}Cs	1.113026006 (39)(118)
^{149}Dy^{w}	4.20 min	#5	^{133}Cs	1.120551852 (809)(817)
^{154}Dy^{u}	3.0 My	#3	^{133}Cs	1.158150408 (77)(139)
^{150}Ho	72 s	#4	^{133}Cs	1.128122043 (183)(215)

tion with the atomic mass of the reference nuclide m_{ref} and taking into account the electron mass m_{e},

$$m = (\nu_{\mathrm{ref}}/\nu) \cdot (m_{\mathrm{ref}} - m_{\mathrm{e}}) + m_{\mathrm{e}}.$$

The contribution of the binding energy of the electron is small compared to the desired accuracy and therefore neglected.

Sources of systematic uncertainties for mass measurements using Penning traps are discussed in various publications [7,10,23,24]. In the mass measurements reported here the aim was an accuracy of $\delta m/m = 1 \cdot 10^{-7}$. At this level of accuracy three principal effects have to be considered [25].

If there is a contamination by another ion species with a mass difference larger than the mass resolution, the frequency shift can easily be detected by plotting the measured frequency as a function of the number of the stored ions [10]. Typically, a relative shift of $\delta\nu/\nu \approx 10^{-7}$ can be detected after a few minutes of measurement time.

Secondly, frequency shifts due to electric and magnetic field imperfections are proportional to the mass difference between the reference nuclide and the nuclide investigated. For the ISOLTRAP experiment these shifts are smaller than $2 \cdot 10^{-9}$/amu [25]. Since the mass difference between the unstable nuclides investigated and the reference nuclide is less than 31 amu, the contribution of such a frequency shift is well below $\delta\nu/\nu \approx 10^{-7}$.

Finally one has to consider the temporal variation of the magnetic field. Typically, a day-night shift of $\delta B/B \approx 10^{-7}$ is observed [25]. Thus their contribution to the systematic uncertainty can be kept well below the desired accuracy if the magnetic field is calibrated every few hours.

The total contribution of all three systematic uncertainties mentioned is less than $1 \cdot 10^{-7}$. Hence it is assumed that a value of $\delta\nu/\nu = 1 \cdot 10^{-7}$ for the total systematic uncertainty is a conservative estimate that includes all systematic effects. For most of the nuclides investigated the statistical uncertainty of the frequency determination is typically of the order of a few 10^{-8}. The total uncertainty is obtained by adding the statistical and the systematic uncertainty quadratically.

3.2.2 Frequency ratios

The frequency ratios of the nuclides investigated are presented in column 5 of table 2 together with their statistical uncertainty (first bracket) and their total uncertainty (second bracket). They are the result of two thesis works [19,20], and most of them have already been published in a proceeding [21]. Some of the given frequency ratios represent an average. In such a case the nuclide has been investigated in more than one beam time. The frequency ratios for these nuclides as determined in each beam time are given in table 3. Even within the statistical uncer-

Table 3. Frequency ratios of nuclides which have been measured in more than one beam time. The nuclides are listed in column 1. ^{137}Sm is a special case (see text). The frequency ratios measured in the individual beam times are given in columns 2-4 and only the statistical errors are given. The weighted mean values are listed in column 5 as the final results which are also given in table 2.

Nuclide	Frequency ratio ν_{ref}/ν			
	Run #3	Run #4	Run #5	Average
^{134}Nd		1.007624574 (17)	1.007624687 (77)	1.007624579 (17)
^{138}Nd		1.037669795 (24)	1.037669803 (77)	1.037669795 (23)
^{143}Pm	1.075282978 (47)		1.075282966 (38)	1.075282971 (29)
^{137}Sm^{y}		1.030259324 (38)	1.030259294 (33)	1.030259307 (25)
^{138}Sm		1.037754800 (22)	1.037754692 (37)	1.037754773 (19)
^{139}Sm	1.045271827 (19)	1.045271755 (54)		1.045271819 (18)
^{142}Sm	1.067790900 (16)	1.067790978 (64)		1.067790904 (16)
^{143}Eu	1.075353533 (26)		1.075353548 (16)	1.075353544 (14)
^{148}Dy		1.113026053 (66)	1.113025980 (49)	1.113026006 (39)

tainty of a few 10^{-8} good agreement is observed between the results obtained in different beam times for almost all nuclides.

The nuclides in table 2 or 3 marked by u, v, w, x, y, z are special cases that will be discussed in appendix B.1. For all other nuclides contamination by a nuclide with a mass difference larger than $\Delta m \geq 200\,\mathrm{keV}$ can be excluded, and there exists no indication for contamination by a nuclide with a smaller mass difference.

3.2.3 Assignment of the measured frequency ratios to isomeric and ground states

If the production ratio of long-lived isomeric and ground states is much different from unity only one of the two states is observed as a resonance signal in the precision trap. One then has to determine which state has been investigated. The other state, if it is produced, has to be treated as a contamination which possibly leads to a frequency shift of the state investigated (see section 2.2).

In order to make an unambiguous assignment for the state investigated, the results of the γ-measurements performed in run #5 were used for some of the nuclides investigated. For other nuclei an assignment can be made if one considers the spins and half-lives of the two states. For some nuclides, where the half-lives of the states were different, a delay time was introduced after collection of the ISOLDE beam in the secondary ion source system of ISOLTRAP to let the shorter-lived state decay. For details on the relative production ratios and the assignment, see appendix B.2.

4 Mass evaluation and results

Within this work an atomic mass evaluation similar to [2, 27] has been performed. A description of the procedure of such a mass evaluation can be found in [2,27]. Such an evaluation takes into account all known information on experimental mass values (input data). A least-squares adjustment is performed on the input data and one obtains atomic mass values as a result. Since the adjustment uses linear equations, the frequency ratios determined by ISOLTRAP have to be converted (see appendix C.1). Only the treatment of the input data and the results of the mass evaluation will be presented here.

4.1 Treatment of all input data

Aside from the experimental results of this work the only input data addressed are those requiring special treatment. All other input data are used as in the 1993 atomic mass evaluation (AME93) [2] and the recent update of 1995 (AME95) [27]. It should be mentioned that preliminary results of run #3 were included in the AME95. Those data are superseded by the final results as given in this publication.

In the ISOLTRAP measurements, masses of several nuclides have been determined experimentally for the first time. This is the case for the nuclides ^{123}Ba, ^{133}Pr, ^{134}Pr, ^{132}Nd, ^{134}Nd, ^{137}Pm, ^{136}Sm and ^{138}Sm. ^{134}Nd and ^{134}Pr were already connected via an experimental Q_{β}-value [29], but there existed no link to a nuclide with known mass. Two other nuclides ^{130}Nd and ^{135}Nd will be treated separately (see below).

There are also nuclides for which the existing experimental data were replaced by values estimated from systematic trends. These are cases where the experimental values are in strong conflict with the trend of neighboring masses values ("... nuclei for which masses estimated from systematic trends are thought better than the experimental masses." [27]). The data presented in this work clarify this unsatisfactory situation for the nuclides ^{138}Nd, ^{138}Pm, ^{139}Eu and ^{150}Ho.

For many nuclides studied in this work mass values were already known. For some nuclei no discrepancies to the existing data were observed and the accuracy of the ISOLTRAP is comparable to the accuracy of the existing

Table 4. Result of the atomic mass evaluation. The selected nuclides and their spins are listed in columns 1 and 2. The mass excess values from two least-squares adjustments are given in column 3 (without Penning trap data) and 4 (with Penning trap data). The differences between the two adjustments are given in column 5. Values estimated from systematic trends are marked by #. Column 6 lists the direct influence of the Penning trap on the mass excess values in column 4. A quantity v/s (column 7) describes the deviation between the Penning trap data and the result of the adjustment. Marked by "exp." in column 8 are those nuclides which are now determined experimentally.

Nuclide	I	Mass excess (keV)		Δ (keV)	Infl.(%)	v/s	note
		AME95 without PT	AME95 with PT				
^{133}Cs	$7/2^+$	−88075.7(3.0)	−88076.0(2.8)	0.2	5	−0.3	
^{123}Ba	$5/2^+$	−75591.0(298.0)#	−75659.7(12.4)	−68.7	100	0.0	exp.
^{125}Ba	$1/2^+$	−79530.7(250.1)	−79665.4(12.4)	−134.7	100	0.0	
^{127}Ba	$1/2^+$	−82789.9(100.4)	−82818.8(12.4)	−28.9	100	0.0	
^{131}Ba	$1/2^+$	−86693.4(6.9)	−86692.4(6.2)	1.0	20	−0.4	
^{137}La	$7/2^+$	−87126.7(47.8)	−87102.5(13.4)	24.2			
^{136}Ce	0^+	−86495.2(47.8)	−86471.0(13.3)	24.2			
^{137}Ce	$3/2^+$	−85904.6(47.8)	−85880.4(13.3)	24.2			
^{133}Pr	$3/2^+$	−78059.0(196.0)#	−77944.2(14.2)	114.8	100	0.0	exp.
^{134}Pr	2^-	−78551.0(298.0)#	−78507.2(15.2)	43.8	100	0.0	exp.
^{135}Pr	$3/2^+$	−80910.4(150.4)	−80939.2(13.3)	−28.8	100	0.0	
^{136}Pr	2^+	−81368.9(51.0)	−81334.8(12.4)	34.0	75	−0.4	
^{137}Pr	$5/2^+$	−83202.6(48.8)	−83180.3(12.0)	22.3	70	−0.2	
^{130}Nd	0^+	−66341.0(503.0)#	−66509.3(120.9)	−168.3	100	0.0	exp.
^{132}Nd	0^+	−71613.0(298.0)#	−71399.1(48.5)	213.9	100	0.0	exp.
^{134}Nd	0^+	−75781.0(334.0)#	−75646.6(13.3)	134.4	100	0.0	exp.
^{135}Nd	$9/2^-$	−76159.0(205.0)#	−76222.5(23.2)	−63.5	100	0.0	exp.
^{136}Nd	0^+	−79157.9(56.8)	−79200.5(13.3)	−42.6	100	0.0	
^{137}Nd	$1/2^+$	−79512.6(72.8)	−79584.3(13.0)	−71.7	95	0.4	
^{138}Nd	0^+	−82037.0(201.0)#	−82021.3(13.3)	15.7	100	0.0	exp.
^{139}Nd	$3/2^+$	−82042.1(50.7)	−82018.4(27.3)	23.7			
^{134}Pm	5^+	−66611.0(389.0)#	−66476.6(200.4)	134.4			exp.
^{135}Pm	$5/2^+$	−70219.0(323.0)#	−70282.0(251.0)#	−63.0			
^{135m}Pm	$11/2^-$	−70119.0(254.0)#	−70182.5(151.8)	−63.5			exp.
^{136}Pm	5^+#	−71307.9(207.9)	−71350.5(200.4)	−42.6			
^{136m}Pm	2^+	−71068.0(240.0)#	−71072.3(93.2)	−4.3	100	0.0	exp.
^{137}Pm	$5/2^+$	−73856.0(135.0)#	−74078.1(13.3)	−222.1	100	0.0	exp.
^{137m}Pm	$11/2^-$	−73855.6(90.9)	−73927.2(56.0)	−71.7			
^{138}Pm	3^+	−75037.0(320.0)#	−74915.9(13.3)	121.1	100	0.0	exp.
^{138m}Pm	1^+	−74954.0(207.0)#	−74938.7(53.2)	15.3			exp.
^{139}Pm	$5/2^+$	−77537.8(58.4)	−77506.2(13.9)	31.5	95	−0.1	
^{140m}Pm	1^+	−77993.4(72.6)	−77780.5(15.2)	212.9	100	0.0	
^{141}Pm	$5/2^+$	−80474.9(27.2)	−80521.0(13.3)	−46.1	87	0.5	
^{143}Pm	$5/2^+$	−82970.5(3.7)	−82970.0(3.6)	0.5	U	0.4	
^{136}Sm	0^+	−66788.0(401.0)#	−66806.0(14.2)	−18.0	100	0.0	exp.
^{137}Sm	$9/2^-$	−67955.6(114.7)	−67946.0(13.3)	9.5	100	0.0	
^{138}Sm	0^+	−71222.0(298.0)#	−71501.0(13.3)	−279.0	100	0.0	exp.
^{139}Sm	$1/2^+$	−72067.8(121.1)	−72383.9(13.3)	−316.2	100	0.0	
^{140}Sm	0^+	−75030.3(301.5)	−75458.3(14.2)	−428.0	100	0.0	
^{141}Sm	$1/2^+$	−75946.1(12.2)	−75945.8(8.7)	0.3	40	0.3	
^{142}Sm	0^+	−78988.2(15.4)	−78994.7(10.2)	−6.5	57	0.4	
^{143}Sm	$3/2^+$	−79527.9(4.1)	−79527.0(4.0)	0.9	U	0.1	
^{139}Eu	$11/2^-$	−65048.0(193.0)#	−65401.5(15.2)	−353.5	100	0.0	exp.
^{140}Eu	1^+	−66560.3(305.6)	−66988.3(52.0)	−428.0			
^{141}Eu	$5/2^+$	−69968.4(28.3)	−69931.4(12.7)	37.0	79	−0.8	
^{142m}Eu	8^-	−70825.9(39.0)	−70862.5(14.2)	−36.6	100	0.0	

Table 4. (*Continued*).

Nuclide	I	Mass excess (keV)		Δ (keV)	Infl.(%)	v/s	note
		AME95 without PT	AME95 with PT				
^{143}Eu	$5/2^+$	−74289.9(26.4)	−74246.6(12.3)	43.3	84	−0.6	
^{144}Eu	1^+	−75661.5(17.6)	−75637.1(12.0)	24.3	54	−1.3	
^{145}Eu	$5/2^+$	−78002.1(4.3)	−78001.5(4.2)	0.6	U	−0.7	
^{146}Eu	4^-	−77128.0(7.2)	−77126.2(6.5)	1.8	19	−0.5	
^{147}Eu	$5/2^+$	−77555.1(3.6)	−77554.6(3.6)	0.5	U	0.5	
^{148}Eu	5^-	−76239.3(17.6)	−76308.5(13.0)	−69.3	83	0.2	
^{149}Eu	$5/2^+$	−76451.5(4.7)	−76451.1(4.7)	0.4	U	−1.3	
^{151}Eu	$5/2^+$	−74663.0(2.9)	−74662.6(2.9)	0.4	U	−0.7	
^{153}Eu	$5/2^+$	−73377.3(2.9)	−73377.0(2.9)	0.3	U	−0.9	
^{148}Tb	2^-	−70515.4(30.5)	−70530.3(15.7)	−14.9			
^{148}Dy	0^+	−67833.4(32.1)	−67850.0(13.8)	−16.6	82	0.3	
^{149}Dy	$7/2^-$	−67688.0(11.1)	−67687.3(11.1)	0.7	U	−0.4	
^{154}Dy	0^+	−70400.4(8.7)	−70401.8(7.8)	−1.3	18	0.6	
^{150}Ho	2^-	−62082.0(100.0)#	−61950.1(27.2)	131.9	100	0.0	exp.
^{152}Ho	2^-	−63583.3(30.6)	−63598.2(15.8)	−14.9			
^{149}Er	$1/2^+$	−53864.0(471.0)#	−53881.0(470.0)#	−17.0			
^{150}Er	0^+	−57974.0(101.0)#	−57842.1(31.0)	131.9			exp.
^{152}Er	0^+	−60474.1(32.2)	−60490.7(13.9)	−16.6			
^{156}Er	0^+	−64259.1(73.7)	−64274.1(68.9)	−14.9			
^{151}Tm	$11/2^-$	−50828.0(135.0)#	−50696.0(94.0)#	132.0			
^{151m}Tm	$1/2^+$	−50783.0(134.0)#	−50651.3(93.0)	131.7			exp.
^{154}Tm	2^-	−54564.0(112.0)#	−54431.7(56.9)	132.3			exp.
^{156}Tm	2^-	−56814.7(58.6)	−56829.7(52.4)	−14.9			
^{151}Yb	$1/2^+$	−41685.0(317.0)#	−41553.2(301.6)	131.8			exp.
^{154}Yb	0^+	−50075.0(101.0)#	−49943.0(31.1)	132.0			exp.
^{156}Yb	0^+	−53237.6(33.0)	−53254.3(15.7)	−16.6			
^{155}Lu	$1/2^+$	−42632.0(134.0)#	−42500.2(92.9)	131.8			exp.
^{155m}Lu	$11/2^-$	−42606.0(135.0)#	−42474.0(94.0)#	132.0			
^{155n}Lu	$25/2^-$	−40828.0(144.0)#	−40696.0(107.0)#	132.0			
^{158}Lu	2^-	−47349.0(123.0)#	−47216.6(75.7)	132.4			exp.
^{158}Hf	0^+	−42246.0(101.0)#	−42114.6(31.3)	131.4			exp.
^{160}Hf	0^+	−45910.0(33.1)	−45926.7(16.0)	−16.6			
^{159}Ta	$3/2^+$	−34545.0(124.0)#	−34413.2(78.2)	131.8			exp.
^{159m}Ta	$11/2^-$	−34436.0(135.0)#	−34304.0(94.0)#	132.0			
^{162}Ta	3^+	−39917.0(132.0)#	−39784.7(90.8)	132.3			exp.
^{162}W	0^+	−34147.0(101.0)#	−34015.2(31.4)	131.8			exp.
^{164}W	0^+	−38206.4(33.2)	−38223.0(16.1)	−16.6			
^{163}Re	$1/2^+$	−26112.0(114.0)#	−25980.6(60.2)	131.4			exp.
^{163m}Re	$11/2^-$	−25943.0(135.0)#	−25811.0(94.0)#	132.0			
^{166}Re	low#	−31855.0(142.0)#	−31722.7(103.6)	132.3			exp.
^{166}Os	$3/2^-$#	−25592.0(102.0)#	−25459.8(32.0)	132.2			exp.
^{168}Os	0^+	−29963.5(33.3)	−29980.1(16.4)	−16.6			
^{167}Ir	$1/2^+$	−17193.0(102.0)#	−17060.8(33.5)	132.2			exp.
^{167m}Ir	$11/2^-$	−16971.0(135.0)#	−16839.0(95.0)#	132.0			
^{170}Ir	low#	−23257.0(150.0)#	−23124.8(115.1)	132.2			exp.
^{170}Pt	0^+	−16463.0(102.0)#	−16331.2(32.6)	131.8			exp.
^{172}Pt	0^+	−21074.0(33.6)	−21090.7(16.9)	−16.6			
^{171}Au	$1/2^+$#	−7662.0(247.0)#	−7530.0(227.0)#	132.0			
^{171m}Au	$11/2^-$	−7362.0(144.0)#	−7230.0(107.0)#	132.0			
^{174}Au	low#	−14050.0(150.0)#	−13917.7(115.5)	132.3			exp.
^{176}Hg	0^+	−11724.5(35.1)	−11741.2(19.7)	−16.6			

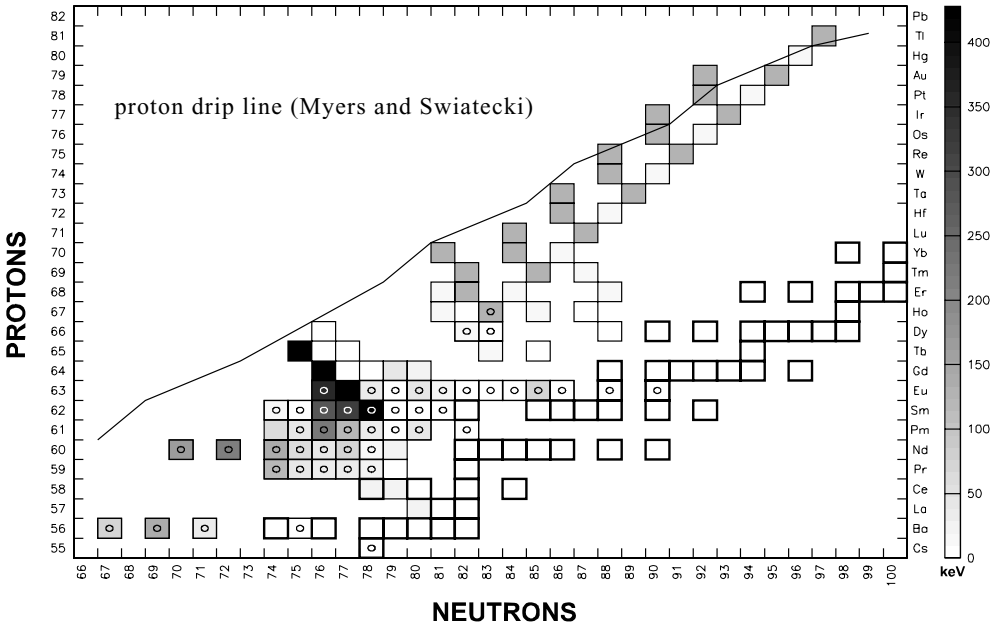

Fig. 5. Result of the far-reaching influence for ISOLTRAP data on the atomic mass evaluation. Different hatching indicates the change of the mass values after the Penning trap data have been added to the other input data of the AME95 [27]. The nuclides measured by ISOLTRAP in this work are marked by a circle. Stable nuclides are surrounded by thick lines. The proton drip line for odd-Z isotopes is indicated as calculated by Myers and Swiatecki [28].

data. In such cases, the Penning trap data are used to improve the accuracy of the corresponding mass values. This was the case for the nuclides ^{133}Cs, ^{131}Ba, ^{137}Pr, ^{137}Nd, ^{139}Pm, ^{141g,141m,142}Sm, ^{141,143,144,146}Eu and ^{148,154}Dy.

To reduce the computing time needed for the least-squares adjustment, insignificant input data are excluded. The authors of AME93 and AME95 mark these data by "Data with much less weight than that of a combination of other data" [27]. Thus, these data have no influence on the mass values which are a result of the atomic mass evaluation. Due to the high accuracy of the ISOLTRAP data, the following input data provided by other experiments became insignificant and were excluded: ^{125}Ba [30], ^{127}Ba [31], ^{135}Pr [32], ^{142m}Eu [33–35] and ^{143}Eu [34, 36]. But also some Penning trap data as presented in this work are insignificant. Those are for ^{143}Pm, ^{143}Sm, ^{145,147,149,151,153}Eu and ^{149}Dy for which more accurate mass values already existed. Thus the ISOLTRAP data for these nuclides do not contribute in the least-squares adjustment but serve to test the reliability of the spectrometer.

Significant discrepancies between data from our work and data from other experiments was observed for the nuclides ^{136}Pr, ^{136}Nd, ^{140m,141}Pm, ^{139,140}Sm and ^{148}Eu. For these nuclides the data from other groups were replaced by the ISOLTRAP values. A detailed discussion of these cases is given in appendix C.2.

Some of the ISOLTRAP input data required different treatment. This was the case for the measurement of ^{130}Nd^{19}F, ^{135}Nd, ^{136}Pm and ^{137}Sm. In the first case the mass of the molecule was measured. Thus, the mass of stable ^{19}F had to be subtracted in the adjustment. For the other nuclei a possible mixture of isomeric and ground states was investigated. A detailed discussion of these cases is given in appendix C.3.

4.2 Results

The result of the atomic mass evaluation is compiled in table 4. Listed are nuclides which fulfill at least one of the following criteria:

- The nuclide was investigated in this work.
- The mass of a nuclide was previously unknown.
- The uncertainty of a mass value has been reduced by a factor of two.
- The mass value was changed by more than one σ.

The nuclides and their spins are listed in columns 1 and 2. Two least-squares adjustments have been performed to show the influence of the Penning trap data on the new mass values. For calculating the mass excess values in column 3, the input data of AME95 have been used [27] but excluding *all* ISOLTRAP data presented in this work. In a second least-squares adjustment the ISOLTRAP results were combined with the input data of AME95 as discussed in section 4.1. The mass excess values resulting from this adjustment are presented in column 4. The differences between the results of both adjustments are listed in column 5. Column 6 lists the direct influence percentage of the Penning trap data on the mass excess values given in column 4. In cases where the mass value is determined by the Penning trap result only, the influence is marked by "100". If the ISOLTRAP data were insignificant, the influence is marked by "U". Other nuclides listed have not been investigated with ISOLTRAP but it can be

Table 5. Excitation energies and assignment to isomeric and ground states as a result of the atomic mass evaluation. The first column lists the nuclides. The spins and half-lives are taken from NUBASE [22] and listed in the following columns. The excitation energy of the isomer is given in column 6. If the excitation energy is negative, a "X" in the last column indicates nuclei for which an inversion of the assignment is suggested. Values estimated from systematic trends are marked by #.

Nuclide	Ground state		Isomeric state			Inversion
	Spin I	$T_{1/2}$	Spin I	$T_{1/2}$	ΔE (keV)	
^{134}Pr	2^-	17(2) min	5^-	11# min	−40(220)	X
^{136}Pm	5^+	107(6) s	2^+	47(2) s	280(220)	
^{137}Pm	$5/2^+$#	2# min	$11/2^-$	2.4(1) min	150(60)	
^{138}Pm	5^-	3.24(5) min	1^+	10.2(2) s	−20(50)	X
^{140}Pm	1^+#	9.2(2) s	8^-	5.95(5) min	650(30)	
^{142}Eu	1^+	2.4(2) s	8^-	1.223(8) min	490(30)	
^{150}Ho	2^-	76.8(1.8) s	9^+	23.3(3) s	−10(60)	

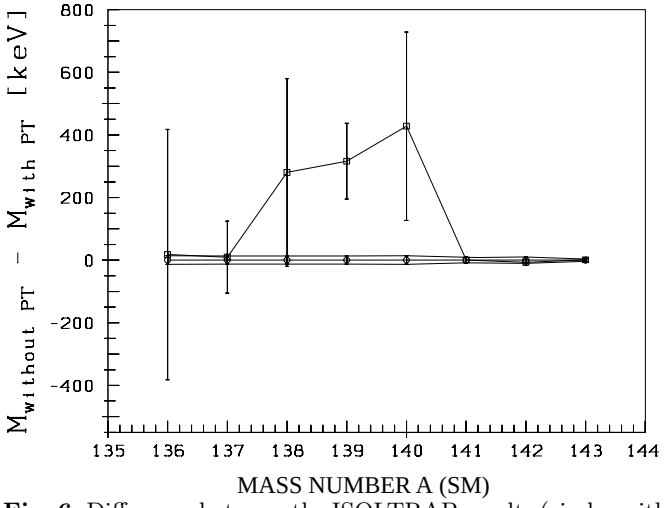

Fig. 6. Difference between the ISOLTRAP results (circles with error band) and the values from the 1995 atomic mass evaluation excluding the ISOLTRAP data (squares with error bars) for the samarium isotopes with $136 \leq A \leq 143$. The solid line through the 1995 values excluding the ISOLTRAP data serves only to guide the eye.

seen that their mass values are influenced indirectly by our data. Column 7 lists a quantity "v/s" for the Penning trap data. This quantity is the deviation between the Penning trap data and the result of the adjustment normalized to the total uncertainty of the ISOLTRAP data. In many cases mass values that were unknown are determined experimentally now that the ISOLTRAP data have been included. These nuclides are indicated by "exp." in column 8.

Figure 5 shows the far-reaching influence of the ISOLTRAP data on the atomic mass evaluation. Plotted are the changes of the mass values that result after the ISOLTRAP data have been added to the other input data as used in AME95 [27].

The adjustment also yields excitation energies for isomers and they are presented in table 5. For ^{134}Pr and ^{138}Pm it is suggested that the assignment of the isomeric and ground states be inverted. The excitation energies for ^{134}Pr, ^{136}Pm, ^{137}Pm and ^{150}Ho were only estimated from systematic trends (see table 8) and are now determined experimentally.

4.3 Impact of the ISOLTRAP data

To show the influence and the high accuracy of the ISOLTRAP data fig. 6 is a plot of the difference between the ISOLTRAP results for the isotopic chain of samarium and the values from the AME95 excluding the ISOLTRAP data.

Prior to the ISOLTRAP measurements mass values for the isotopes ^{136}Sm and ^{138}Sm were only estimated from systematic trends. The mass values for the remaining isotopes were determined by Q_β-values or reaction data. There is a good agreement between the ISOLTRAP data and the previous experimental data for the three isotopes closest to stability. This indicates that the assumptions concerning the systematic uncertainty are correct (see section 3.2.1). However, large discrepancies are observed for the isotopes ^{139,140}Sm where the mass values were previously only known from links provided by Q_β-measurements.

Due to known Q-value links, mass measurements with an accuracy of $\delta m/m \approx 1 \cdot 10^{-7}$, as routinely achieved with ISOLTRAP, can have a large impact on mass values other than those measured directly. The case of ^{150}Ho will be discussed as an example. As can be seen from fig. 7 its mass value is connected to those of 19 nuclides via experimental Q-values including α-decay chains up to ^{171,174}Au and ^{170}Pt.

An experimental Q-value [34] for ^{150}Ho, which resulted in a mass excess of $ME = -62760(100)$ keV given in AME93 [2], was rejected in AME95 [27]. Thus, no mass link existed between these nuclei and the valley of stability. This unsatisfactory situation is now remedied by the ISOLTRAP measurement on ^{150}Ho. The measured frequency ratio results in a mass excess of $ME = -61950(27)$ keV. This justifies the early rejection of the old experimental datum which differs by 810 keV from the ISOLTRAP value. The ISOLTRAP measurement therefore not only gives an accurate experimental mass value for ^{150}Ho but also anchors the masses for all 19 nuclides linked to it.

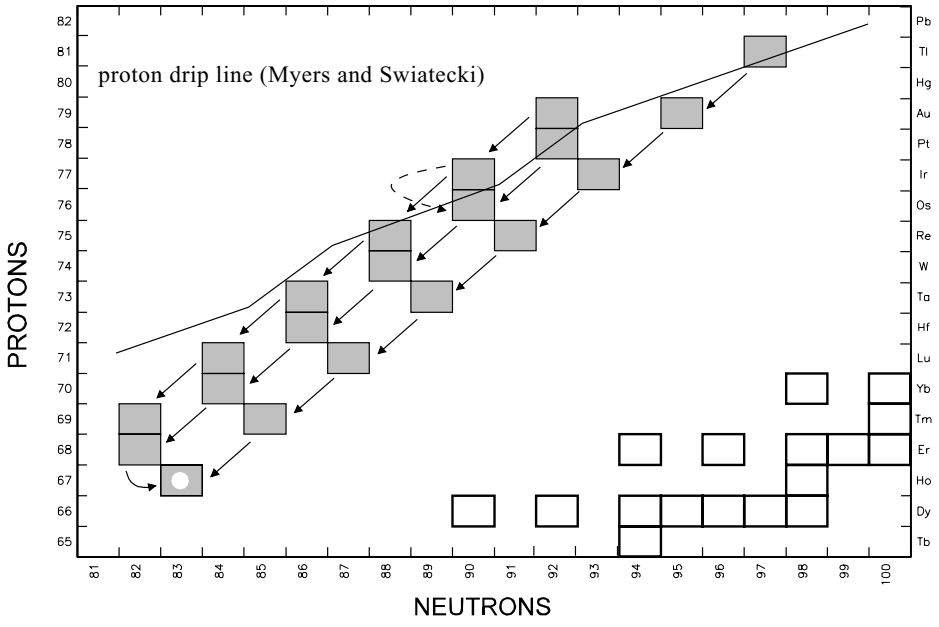

Fig. 7. Connection between mass values around ^{150}Ho (indicated by a white circle). The connections shown are Q_α-measurements (solid straight lines), one Q_β-measurement (solid curved arrow) and a Q_p-measurement of ^{167}Ir (dashed curved arrow). Stable nuclides are marked by white squares. The proton drip line for odd-Z isotopes is indicated as calculated in [28].

Table 6. Comparison of mass values known from other experiments with mass values calculated from experimental results of this work. Shown in column 1 are nuclides for which the mass values have already been determined by other experiments with an accuracy of $1 \cdot 10^{-7}$ or better. These mass values are listed in column 2 (see text). Given in column 3 are mass values resulting from experimental results of this work (see text). The differences are given in column 4.

Nuclide	Mass excess (keV)		Δm (keV)
	AME95 without PT	Penning Trap only	
^{133}Cs	−88075.7(3.0)	−88072.3 (13.0)	3.4
^{131}Ba	−86693.4(6.9)	−86687.3 (13.5)	6.1
^{143}Pm	−82970.5(3.7)	−82975.2 (14.2)	−4.7
^{141}Sm	−75946.1(12.2)	−75946.6 (13.9)	−0.5
^{143}Sm	−79527.9(4.1)	−79527.6 (14.4)	0.3
^{145}Eu	−78002.1(4.3)	−77989.3 (15.9)	12.8
^{146}Eu	−77128.0(7.2)	−77118.8 (14.8)	9.2
^{147}Eu	−77555.1(3.6)	−77561.8 (15.5)	−6.7
^{149}Eu	−76451.5(4.7)	−76429.4 (16.0)	22.1
^{151}Eu	−74663.0(2.9)	−74652.1 (14.8)	10.9
^{153}Eu	−73377.3(2.9)	−73362.7 (15.4)	14.6
^{154}Dy	−70400.4(8.7)	−70410.9 (17.6)	−10.5

4.4 Accuracy of the ISOLTRAP data

As described in section 3.2.1, a systematic uncertainty of $1 \cdot 10^{-7}$ is used to cover all effects possibly leading to a systematic shift of the ions cyclotron frequency. For most of the nuclides investigated this systematic uncertainty is larger than the statistical uncertainty and contributes most to the total uncertainty of a measurement.

It must be stated that the results presented in this work are not only precise but also accurate. In order to confirm this it is assumed that those nuclides given in the AME95 with an accuracy of $1 \cdot 10^{-7}$ or better can be used as an accurate mass meter on this level of accuracy.

Thirteen nuclides known with this accuracy have been investigated. Table 6 shows a comparison between the experimental mass values of this work with the result of the AME95 without the Penning trap data. The experimental mass values from this work were determined from the frequency ratios and the mass values of the reference nuclides as given in AME95 (see section 3.2.1). The nuclide ^{149}Dy was excluded from the comparison since the uncertainty of the ISOLTRAP value is untypically large. The weighted mean and its standard deviation of the difference between the AME95 and the ISOLTRAP values is

$$\Delta m = +4.8(10.4)\,\text{keV}. \quad (2)$$

Within the quoted uncertainty no systematic deviation from the ISOLTRAP data to other better known mass values can be observed. This demonstrates the reliability of the ISOLTRAP mass spectrometer. It further confirms that the estimated systematic uncertainty of $1 \cdot 10^{-7}$ takes reasonably into account all the uncorrected and possible systematic effects showing up in an on-line run at an accelerator facility.

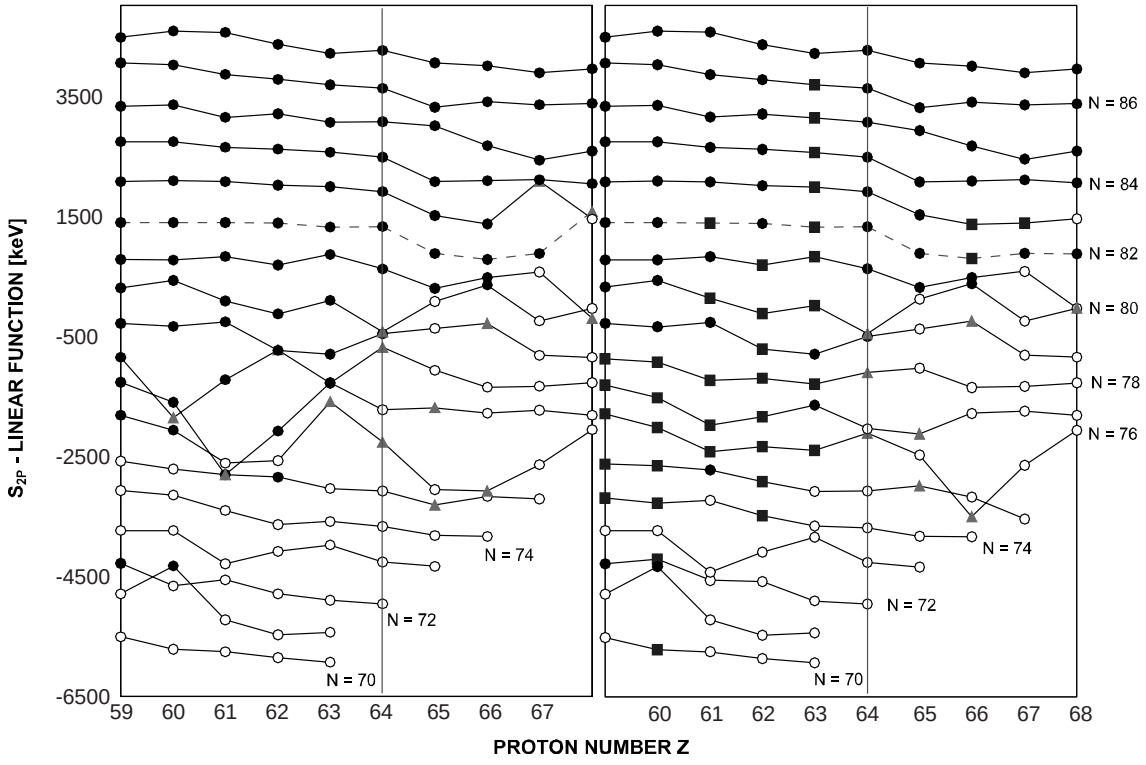

Fig. 8. Two-proton separation energies as a function of proton number for different nuclides. Shown are the values without (left) and including (right) the ISOLTRAP data. The nuclides are marked by squares (mass values measured by ISOLTRAP), solid circles (other experimental mass values), open circles (mass values estimated from systematic trends) and triangles (doubtful experimental value [27]).

5 Discussion of the results of the atomic mass evaluation

5.1 Two-proton and two-neutron separation energies

Since separation energies better illustrate the effect of the binding energies than do mass values they will now be discussed. Figures 8 and 9 show the influence of the ISOLTRAP data on the trend of the two-proton and two-neutron separation energies obtained from the experimental mass values. Shown is the result of the atomic mass evaluation excluding and including the data presented in this work. A linear function has been subtracted in both figures. The graphs can be divided into four quadrants by the neutron shell closure at $N = 82$ and the proton sub-shell closure at $Z = 64$.

For $N \geq 82$ and $Z < 64$ a smooth trend is observed as a function of the proton number. Here, the mass values are well known and the situation does not change significantly after the ISOLTRAP data have been included. This is in contrast to the region of $N < 82$ and $Z \geq 64$ where almost nothing is known.

In the region of $N \geq 82$ and $Z \geq 64$ the proton sub-shell closure can be observed as a decrease of the two-proton separation energy between $Z = 64$ and $Z = 65$. Rather large discontinuities are observed at $Z = 67$ and $Z = 68$ which disappear after the ISOLTRAP data have been included. This is due to the ISOLTRAP measurement of ^{150}Ho. The two-proton separation energies of another 18 nuclides not shown in the graph are also shifted by the same value (see section 4.3).

In the region of $N < 82$ and $Z < 64$ many mass values have been measured for the first time by ISOLTRAP. Some large jumps due to doubtful mass values [27] disappear when the ISOLTRAP data are included. However, a closer look at the two-proton separation energies (fig. 8) around $Z = 61$ yields a deviation from the smooth trend between $N = 76$ and $N = 78$. This trend becomes even more pronounced for the two-neutron separation energies (fig. 9). While the two-neutron separation energies follow an almost straight line for the barium isotopes ($Z = 56$), the separation energies of the rare-earth isotopes with $Z < 64$ show an almost identical behavior, except for the promethium isotopes ($Z = 61$). With N increasing from $N \approx 70$, the separation energies show a "maximum"[2] around $N = 77$, followed by a "minimum" between $N = 77$ and the main shell closure at $N = 82$. This behavior indicates a nuclear structure effect. Often such effects can be correlated to nuclear deformation as has been shown by Barber *et al.* [37] in the early sixties, where a sudden onset of deformation around $N = 90$ for rare-earth isotopes has been indicated by mass measurements. However, the discontinuity for the nuclides with

[2] Deviations from the general trend show up as maxima and minima in the plotted separation energies due to a linear function that has been subtracted.

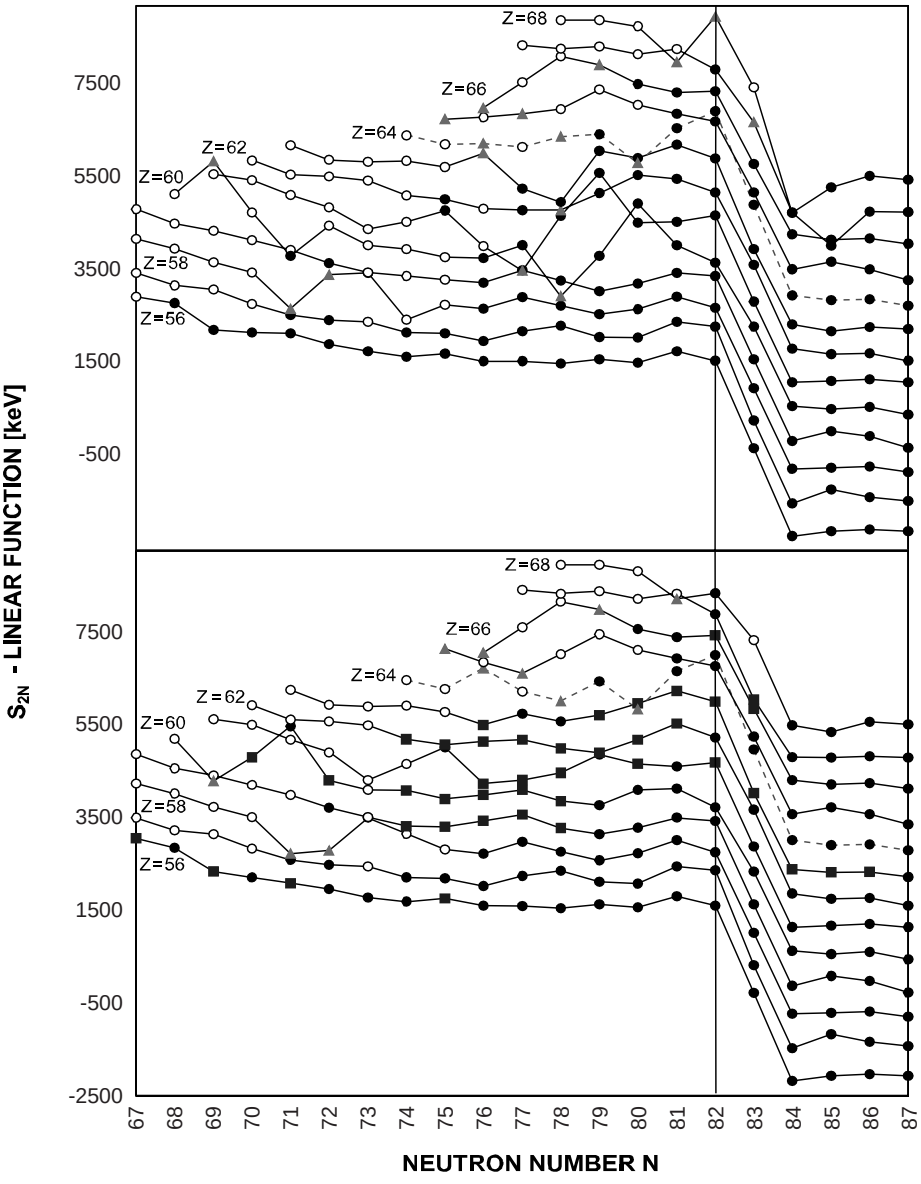

Fig. 9. Two-neutron separation energies as a function of neutron number for different nuclides. Shown are the values without (top) and including (bottom) the ISOLTRAP data. The nuclides are marked by squares (mass values measured by ISOLTRAP), solid circles (other experimental mass values), open circles (mass values estimated from systematic trends) and triangles (doubtful experimental value [27]).

$N \leq 82$ is less pronounced than for the nuclides around $N = 90$.

5.2 Proton separation energies at the drip line

Many nuclides around ^{146}Gd are endpoints of parallel α-decay chains that originate from nuclei in the vicinity of $Z \approx 82$ and hence close to the proton drip line ($S_\mathrm{p} = 0\,\mathrm{keV}$). For most of these α-chains the mass differences between the nuclides have been measured via α-spectroscopy [27]. If the mass values of the nuclides at the individual endpoints are known, the proton separation energies, and from these the proton drip line, can be determined. The mass values of some endpoints are determined or improved by the data presented in this work.

Figure 10 shows the one-proton separation energies and the proton drip line as a function of neutron number for different elements with odd proton number. The proton separation energies for the nuclides of the chain to ^{151}Tm result from Q_α-measurements and from a direct investigation of proton emitters that has been performed in Argonne [38]. For the α-decay chains to ^{149}Ho and ^{150}Ho, the separation energies stem from the atomic mass evaluation 1995 and the experimental data presented in this work. The influence of the data of this work becomes obvious when one compares the ^{150}Ho α-decay chain resulting from this work (solid triangles) to that derived from an earlier mass measurement [36] (see section 4.3) indicated

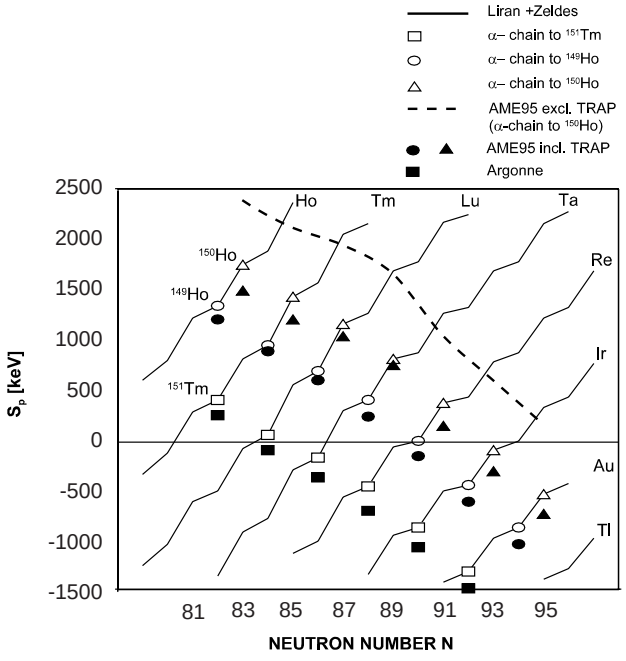

Fig. 10. Proton separation energies as a function of neutron number for different elements. The individual α-decay chains are marked by squares (endpoint ^{151}Tm), circles (endpoint ^{149}Ho) and triangles (endpoint ^{150}Ho). The open symbols on the black lines indicate the values predicted by Liran and Zeldes [40]. Filled symbols indicate the α-chains after the ISOLTRAP data has been added to the atomic mass evaluation 1995. To demonstrate the influence of the ISOLTRAP data, the dashed line indicates S_p values for the α-decay chain to ^{150}Ho, derived from an earlier experimental mass value of this nuclide.

by the dashed line. One can also observe a 300–400 keV shift of the ^{149}Ho line in fig. 10 compared to the one in a similar figure in [39].

As a comparison, the predictions of the mass model of Liran and Zeldes [40] are shown. These predictions are in good agreement with the experimental data. However, the proton separation energies derived from experimental data are slightly lower than predicted, resulting in a narrower valley of stability.

6 Summary and conclusions

Direct mass measurements on short-lived rare-earth isotopes around ^{146}Gd have been performed with ISOLTRAP. Masses of more than 40 nuclides were determined and many of those were measured for the first time. An accuracy of $1 \cdot 10^{-7}$ corresponding to $\delta m \approx 14$ keV has been reached.

The spectrometer was operated with a mass resolving power $m/\Delta m$(FWHM) of $6 \cdot 10^5$ to $3 \cdot 10^6$. The high resolving power of ISOLTRAP allows isomeric and ground states to be distinguished even for very small mass differences, which is very important for the accurate determination of many ground-state masses.

An atomic mass evaluation has been performed taking into account the data presented in this work and the input values of the atomic mass evaluation from 1995. As a result, many nuclides have now been linked to the body of accurate mass data. Furthermore, the far-reaching influence of these precise values has improved mass values of a large number of nuclides, many significantly.

For the nuclei with $N \geq 82$ the data give new information on the position of the proton drip line in the mercury and lead region. For $N < 82$ the mass values deviate from the regular trend which indicates the existence of a nuclear structure effect around $76 \leq N \leq 78$.

Appendix A. Determination of ISOLDE beam currents from measured γ-line intensities

Measurements of the γ-line intensities of some of the nuclides delivered by ISOLDE have been performed in run #5. From the measured γ-activity and the known relative intensities of the γ-lines of the daughter nucleus, the yield delivered by the ISOLDE mass separator was determined [41]. Table 7 shows the result of these investigations carried out at different temperatures of the ISOLDE target. A change in this temperature affects the time in which an atom diffuses out of the target. Since this diffusion time depends on chemical properties, in many cases one observes a change in the relative amount of the delivered nuclides.

Appendix B. Data analysis

This section gives additional information on the determination of the cyclotron frequency ratios and their assignment to nuclides.

Appendix B.1. Special cases

For few of the nuclides investigated a possible frequency shift due to contamination by another nuclide cannot be excluded. This was the case for the nuclides ^{130}Nd^{19}F, ^{135}Nd, ^{136}Pm, ^{137}Sm and ^{149,154}Dy marked by x, y, z, u, v and w in table 2. Possible contaminations are isobars, isomers and side-bands of fluorines and oxides of the same mass number.

Since a separation of the ground and isomeric states of ^{135}Nd was not attempted, it is possible that it was a mixture of both states that was measured. For ^{136}Pm the line shape does not indicate a contamination with a mass difference larger than its line width. However, the statistics are not sufficient to exclude this possibility. For ^{137}Sm systematic trends indicate the existence of a long-lived isomer (see appendix C.3) with small excitation energy. A resolution of two such possible states was not attempted. For ^{154}Dy the poor statistics do not allow the exclusion of the contamination by the isobar ^{154}Tb. However, due to

Table 7. Overview of the γ-measurements performed in run #5. Listed are the different nuclides (column 1), literature values of their half-lives [22] (column 2) and the energy of the γ-line used for identification (column 3). The yields delivered by ISOLDE (column 4) are calculated from the measured γ-intensity [41]. The uncertainty of the yields is in the order of 50%. The heating current of the ISOLDE target (column 5) and the corresponding temperature (column 6) are given as well.

Nuclide	$T_{1/2}$	E_γ (keV)	Yield (atoms/s)	I_{Target} (A)	T_{Target} (°C)
^{139g}Sm	154 s	273.7	$4.5 \cdot 10^6$	720	1950
^{139m}Sm	10.7 s	190.1	$2.9 \cdot 10^5$	·	·
^{139}Pm	4.15 min	402.8	$1.6 \cdot 10^6$	·	·
^{150}Dy	7.17 min	397.2	$6.6 \cdot 10^5$	·	·
^{150}Tb	3.48 h	638.1	$4.2 \cdot 10^6$	·	·
^{139g}Sm	154 s	273.7	$8 \cdot 10^6$	780	2060
^{139m}Sm	10.7 s	190.1	$1.1 \cdot 10^6$	·	·
^{139}Pm	4.15 min	402.8	$3.5 \cdot 10^6$	·	·
^{150}Ho	76.8 s	803.7	$1.6 \cdot 10^4$	·	·
^{150}Dy	7.17 min	397.2	$1.9 \cdot 10^6$	·	·
^{150}Tb	3.48 h	638.1	$9.3 \cdot 10^6$	·	·
^{139}Pm	4.15 min	402.8	$3.5 \cdot 10^6$	·	·
^{150}Ho	76.8 s	803.7	$1.6 \cdot 10^4$	·	·
^{150}Dy	7.17 min	397.2	$1.9 \cdot 10^6$	·	·
^{150}Tb	3.48 h	638.1	$9.3 \cdot 10^6$	·	·
^{139g}Sm	154 s	273.7	$2 \cdot 10^7$	820	2100
^{139m}Sm	10.7 s	190.1	$1.5 \cdot 10^6$	·	·
^{139}Pm	4.1 min	402.8	$3.8 \cdot 10^6$	·	·
^{148}Dy	3.1 min	620.2	$1.7 \cdot 10^6$	·	·
^{148}Tb	1 h	784.4	$2.4 \cdot 10^6$	·	·
^{150}Ho	76.8 s	803.7	$2.8 \cdot 10^4$	820	2100
^{150}Dy	7.17 min	397.2	$9.5 \cdot 10^6$	·	·
^{150}Tb	3.48 h	638.1	$3.6 \cdot 10^7$	·	·
^{151}Ho	35.2 s	527.	$5 \cdot 10^4$	·	·
^{151}Dy	17.9 min	386.1	$2.2 \cdot 10^7$	·	·
^{151}Tb	17.61 h	251.9	$2.4 \cdot 10^8$	·	·
^{151m}Tb	25 s	49.5	$4.8 \cdot 10^6$	·	·
^{133}Nd	70 s	164.2	$1 \cdot 10^6$	880	2150
^{133}Pr	6.5 min	134.3	$4 \cdot 10^7$	·	·
^{133m}Ce	4.9 h	130.8	$3.6 \cdot 10^7$	·	·
^{138}Eu	12.1 s	346.7	$> 3.4 \cdot 10^4$	·	·
^{138}Pm	3.2 min	520.9	$2.7 \cdot 10^6$	·	·
^{138}Nd	5.04 h	325.8	trace (?)	·	·
^{139g}Sm	154 s	273.7	$3.4 \cdot 10^7$	·	·
^{139m}Sm	10.7 s	190.1	$4.1 \cdot 10^6$	·	·
^{139}Pm	4.15 min	402.8	$1.7 \cdot 10^7$	·	·
^{140}Sm	14.8 min	140.	$1.3 \cdot 10^8$	·	·
^{140m}Pm	6 min	419.6	$2.2 \cdot 10^6$	880	2150
^{140g}Pm	9.2 s	773.8	not seen	·	·
^{150}Ho	76.8 s	803.7	$1.8 \cdot 10^5$	·	·
^{150}Dy	7.17 min	397.2	$3.1 \cdot 10^7$	·	·
^{150}Tb	3.48 h	638.1	$1.2 \cdot 10^8$	·	·
^{140}Eu	1.5 s	530.7	$1.8 \cdot 10^5$	900	2165
^{140}Sm	14.8 min	140.0	$1.1 \cdot 10^8$	·	·
^{140m}Pm	6 min	419.6	$2 \cdot 10^6$	·	·
^{140g}Pm	9.2 s	773.8	not seen	·	·
^{141m}Eu	2.7 s	96.4	$1.9 \cdot 10^7$	·	·
^{141g}Eu	40.7 s	384.5	$3.8 \cdot 10^7$	·	·
^{141m}Sm	22.6 min	431.8	$7.4 \cdot 10^8$	·	·

Table 7. (*Continued*).

Nuclide	$T_{1/2}$	E_γ (keV)	Yield (atoms/s)	I_{Target} (A)	T_{Target} (°C)
^{141g}Sm	10.2 min	403.9	$3.7 \cdot 10^8$	·	·
^{142m}Eu	1.2 min	556.6	$1.6 \cdot 10^7$	·	·
^{142g}Eu	2.4 s	768.0	not seen	·	·
^{142}Sm	72.5 min	1243.0	not seen	·	·
^{142}Pm	40.5 s	1575.8	$2.2 \cdot 10^7$	·	·
^{143m}Gd	1.9 min	271.9	$2.1 \cdot 10^5$	·	·
^{143g}Gd	39 s	258.8	not seen	·	·
^{143}Eu	2.6 min	107.0	$7.6 \cdot 10^7$	·	·
^{143m}Sm	1.1 min	754.4	$9.6 \cdot 10^6$	·	·
^{143g}Sm	8.8 min	1056.6	$1.4 \cdot 10^8$	·	·
^{144}Eu	10 s	817.7	$3 \cdot 10^7$	·	·
^{144m}Tb	4.25 s	283.9	trace (?)	·	·
^{168m}Lu	6.7 min	198.8	$5 \cdot 10^6$	·	·
^{168}Lu	5.5 min	111.4	$2.3 \cdot 10^5$	·	·
^{176}W(?)	2.5 h	100.2	$5 \cdot 10^4$	·	·
^{176}Ta	8.1 h	1159.3	not seen	·	·
^{176m}Yb	11.4 s	292.9	$1.2 \cdot 10^4$	·	·

the low target temperature used during this measurement, a production of ^{154}Tb by ISOLDE and thus a frequency shift for ^{154}Dy is very unlikely.

The molecule ^{130}Nd^{19}F has been measured with a mass resolution of 600 keV (T_{rf}=300 ms). A contamination of a nuclide with a smaller mass difference can be excluded since the isobar ^{149}Dy has been removed from the precision trap via excitation at its reduced cyclotron frequency. However, a contamination by a nuclide with a larger mass difference can not be excluded due to the small number of detected ions for this nuclide. The statistics of the measurement on ^{130}Nd^{19}F are very poor, thereby rendering it to a *tentative result*.

^{149}Dy was also investigated with a mass resolution of 600 keV. A contamination with a larger mass difference can be excluded from the count-rate dependence and the line shape of the resonance signal. However, during the measurement a contamination of the ISOLDE beam with ^{130}Nd^{19}F, with a mass difference smaller than the line width of the resonance, was overlooked. The cyclotron frequency was therefore the mean cyclotron frequency of the ion cloud [11] $\nu_{\mathrm{c}}(\mathrm{NdF} + \mathrm{Dy}) = 610822.914(69)$ Hz. From this value, knowing the ratio of the number of stored ion of both species, one can obtain the cyclotron frequency of pure Dy ions [42,11]. From the number of detected ions during the measurement of ^{130}Nd^{19}F and ^{149}Dy a ratio $R' = N_{\mathrm{NdF}}/(N_{\mathrm{Dy}} + N_{\mathrm{NdF}}) = 0.31(16)$ is determined. Since the cyclotron frequency of ^{130}Nd^{19}F was measured to be $\nu_{\mathrm{c}}(\mathrm{NdF}) = 610823.98(53)$ Hz, one can correct the measured cyclotron frequency of $\nu_{\mathrm{c}}(\mathrm{NdF} + \mathrm{Dy})$ and obtain the cyclotron frequency of pure ^{149}Dy, $\nu_{\mathrm{c}}(\mathrm{Dy}) = 610822.44(44)$ Hz. This frequency is used to determine the frequency ratio of ^{149}Dy given in table 2.

Appendix B.2. Isomeric or ground-state assignment

Many nuclides around ^{146}Gd have long-lived isomers with excitation energies of 1 MeV or less. Such isomers are produced by ISOLDE and cannot be separated by the cooler trap of ISOLTRAP. For most nuclei the production of ground and isomeric states is different, and one has to determine experimentally whenever possible, or at least to estimate, whether the ground state, the isomeric state, or a mixture of the two is being delivered. In the last case, one of the two states has to be regarded as a contamination which possibly may cause a frequency shift of the state that is investigated (see section 2.2).

Appendix B.2.1. Criteria for identification

The γ-measurements performed during run #5 give information on the relative amounts of isomeric and ground states in the ISOLDE beam. If their mass difference is larger than the line width of the resonance signal, the measured cyclotron frequency can then be assigned to the isomeric or the ground state. If the mass difference between the two states is smaller, the γ-measurements yield information on the possible admixture of the less dominant state.

For nuclei where no γ-measurements have been performed, the relative amount of isomeric and ground states can be estimated via their spins and half-lives. Rare-earth isotopes are produced by spallation of the target material tantalum. Empirically it has been shown that this production mechanism favors the state with low spin [43,44]. Before the produced nuclides are ionized in the ion source they have to diffuse out of the target. Since the diffusion times of rare-earth isotopes can be up to minutes, depending on the target temperature and the element, the state with longer half-life is favored during the diffusion process.

Table 8. Half-lives and spins of the nuclides investigated, for which more than one long-lived state exist. The first column lists the nuclides. The spins, half-lives, and excitation energies are taken from NUBASE [22] and listed in the following columns. The last column gives the ratio R of isomeric to ground states for the stored ions in the precision trap as used in the data analysis of this work. If a ratio is given as "?", the assignment was not done in the data analysis but the value given in brackets was used in the atomic mass evaluation (see text). Values estimated from systematic trends are marked by #.

Nuclide	Ground State		Isomeric State			R
	Spin I	$T_{1/2}$	Spin I	$T_{1/2}$	ΔE (keV)	
^{127}Ba	$1/2^+$	12.7(4) min	$7/2^-$	1.9(2) s	88.33(12)	0.0
^{131}Ba	$1/2^+$	11.50(6) d	$9/2^-$	14.6(2) min	187.14(12)	0.0
^{134}Pr	2^-	17(2) min	5^-	11# min	0(200)#	0.0
^{135}Nd	$9/2^-$	12.4(6) min	$1/2^+$	5.5(5) min	65.1(5)	?(1.0)
^{137}Nd	$1/2^+$	38.5(1.5) min	$11/2^-$	1.60(15) s	519.6(5)	0.0
^{136}Pm	5^+	107(6) s	2^+	47(2) s	240(240)#	?(∞)
^{137}Pm	$5/2^+$#	2# min	$11/2^-$	2.4(1) min	0(100)#	0.0
^{138}Pm	5^-	3.24(5) min	1^+	10.2(2) s	80(260)	0.0
^{139}Pm	$5/2^+$	4.15(5) min	$11/2^-$	180(20) ms	188.7(3)	0.0
^{140}Pm	1^+#	9.2(2) s	8^-	5.95(5) min	440(70)	∞
^{137}Sm	$9/2^-$	45(1) s	$1/2^+$#	20# s	180(50)#	?(0.0)
^{139}Sm	$1/2^+$	2.57(10) min	$11/2^-$	10.7(6) s	457.8(4)	≤ 0.1
^{141}Sm	$11/2^-$	22.6(2) min	$1/2^+$	10.2(2) min	175.8(3)	2.0
^{143}Sm	$3/2^+$	8.83(1) min	$11/2^-$	66.2 s	754.0(2)	≤ 0.1
			$23/2^-$	30(3) ms	2794.7(5)	
^{141}Eu	$5/2^+$	40.7(5) s	$11/2^-$	2.7(3) s	96.4(1)	≤ 0.1
^{142}Eu	1^+	2.4(2) s	8^-	1.223(8) min	520(50)	∞
^{150}Ho	2^-	76.8(1.8) s	9^+	23.3(3) s	120(110)#	0.0
^{149}Dy	$7/2^-$	4.20(14) min	$27/2^-$	490(15) ms	2661.1(4)	0.0

During a measurement the nuclides delivered by ISOLDE are first collected on the filament of the reionizer of the ISOLTRAP spectrometer and then desorbed and reionized by heating the filament. If the half-life of the nuclide investigated is longer than that of a possibly contaminating nuclide, an additional delay between collecting and desorption can be used to discriminate between the two states by letting the unwanted species decay. This method also enables a rough estimate of the half-life of the nuclide investigated.

Appendix B.2.2. Assignment

Table 8 lists those nuclides where long-lived states are known [22] together with their spins, half-lives, excitation energies, and the ratio R between isomeric and ground states as used in the data analysis of this work. This assignment was then used for the mass evaluation, except for ^{135}Nd, ^{136}Pm and ^{137}Sm, where the values of R given in brackets were used.

^{127,131}Ba, ^{137}Nd, ^{139}Pm and ^{149}Dy
The ground states of these nuclides were investigated. The isomers can be excluded due to higher spins and shorter half-lives.

^{134}Pr
It is assumed that the ground state is produced due to its longer half-life and lower spin.

^{135}Nd^z
No clear assignment to one of the states is possible. Due to its low spin, the isomeric state should be produced more abundantly in the target but the longer-lived ground state is favored during the diffusion out of the target. Since the excitation energy $\Delta E = 65.1(5)$ keV of the isomer is smaller than the width of the resonance curve, it is impossible to detect whether or not the ion sample is a mixture of both states.

^{136}Pm^x
As for the case of ^{135}Nd there is no assignment possible to either one of the two possible states. It is also not clear which of the two states is the ground state. Within the statistics of this measurement it cannot be decided whether or not the line shape of the measured cyclotron curve deviates from the theoretically expected shape.

^{137}Pm
The spin of the ground state is estimated to be smaller than the one of the isomeric state. Thus it is assumed that the ground state is predominantly produced.

^{138}Pm
The longer-lived state with spin $I = 5^-$ has been investigated. During several measurements a delay of 1 min was introduced between collection of the ISOLDE beam and first heating of the reionizer. The presence of the shorter-lived state ($T_{1/2} = 10.2$ s) should have been detected. None was.

^{140m}Pm
The longer half-life and the measured intensities of the γ-lines indicate that the isomer has been investigated. Since the excitation energy $\Delta E = 440(70)$ keV of the isomeric state is larger than the line width, a possible contamination by the ground state would have been detected which was not the case.

^{137}Sm^{y}
Systematic trends suggest an isomeric state with an excitation energy of $\Delta E = 180(50)$ keV (see section C.3). No unambiguous assignment to one of the two states is possible.

^{139}Sm
During runs #3 and #4 the ground state was investigated using a relatively low target temperature. During some of the measurements an additional delay of 1 minute was introduced between the collection of the ions on the foil of the reionizer and the start of the measurement. Therefore the short-lived isomer can be excluded. Since the excitation energy $\Delta E = 457.8(4)$ keV of the isomer is larger than the width of the resonance curve, a contamination by the isomeric state would have been detected if present. The relative production ratio has been determined by measuring the intensities of γ-lines during run #5. These measurements show that the relative amount of the isomeric state is around 10% and thus low. Since the measurements were performed using a small number of stored ions, a shift of the cyclotron frequency of the ions is not expected.

^{141g}Sm and ^{141m}Sm
The excitation energy of the isomer corresponds to the mass difference between the two states. Both states have been resolved in the precision trap. Since less than five ions have been stored at the same time, the motions of the ions decouple and the cyclotron frequencies are not shifted (see section 2.2). The measurement showed that the relative amount of isomeric and ground states is two to one (see fig. 4). This was confirmed by the γ-measurements.

^{143}Sm
Run #3 was aimed at the investigation of the ground state, which was predominantly produced due to its low spin and longer half-life. The excitation energy $\Delta E = 754.0(2)$ keV of the isomer is larger than the line width of the resonance curve so contamination by the isomeric state should have been detected which was not the case. The γ-measurements performed in run #5 showed that the relative amount of the isomeric state was 10% or less. Moreover, the mass measurement performed in run #3 was done at even lower temperature of the ISOLDE target. Thus the relative amount of the isomer during the mass measurement was significantly less than 10%. In addition, a small number of stored ions was used during the measurement. A shift of the cyclotron frequency of the ground state is not expected.

^{141}Eu
The γ-measurements showed that ground and isomeric states are produced with a ratio of two to one. However, since the mass measurements on this nuclide were done at a lower target temperature, it is estimated that the relative amount of the shorter-lived isomeric state during the frequency measurement is less than 10%. The excitation energy of the isomeric state is $\Delta E = 96.4(1)$ keV whereas the linewidth corresponds to $\Delta E \approx 200$ keV. So the isomer must be treated as a contamination of a smaller mass difference. The shift of the cyclotron frequency of the ground state can be calculated as in [42]. The resulting shift would be less than 10 keV and, within the accuracy of the measurement, can be neglected.

^{142m}Eu
Due to its longer half-life, the isomeric state should be predominantly produced. This was corroborated by the γ-measurements. Since the excitation energy $\Delta E = 520(50)$ keV of the isomeric state is larger than the line width, a possible contamination by the ground state should have been detected. None was.

^{150}Ho
During run #4 the ground state was investigated. A contamination by the isomer is unlikely due to its high spin and three times shorter half-life. Moreover, a shift of the cyclotron frequency of the ground state is excluded since, on the average, only one ion was stored at the same time. The γ-measurements performed in run #5 indicated that it was the ground state that is produced by ISOLDE. The beam intensities in run #5 were not sufficient for a frequency determination.

Appendix C. Atomic mass evaluation

This section gives additional information on the treatment of the input data for the atomic mass evaluation. Firstly, the conversion of the measured frequency ratios into linear relations is given. The resolution of conflicts between data of the present work and other works is discussed next. Finally, ISOLTRAP data requiring special treatment are presented.

Appendix C.1. Conversion to linear relations

In this experiment the physical quantities measured are ratios

$$r = \frac{\nu_{\mathrm{ref}}}{\nu} \tag{3}$$

of the cyclotron frequency ν_{ref} of the reference nuclide and the cyclotron frequency ν of the investigated nuclide. The frequency ratios correspond to the mass ratio of the ionic species

$$r = \frac{m - m_{\mathrm{e}}}{m_{\mathrm{ref}} - m_{\mathrm{e}}}, \tag{4}$$

where m and m_{ref} denote the atomic mass of the investigated and reference nuclide, respectively, and m_{e} is the mass of the electron. The binding energy of the valence electron can be neglected.

To use the present results in the standard least-squares method for the evaluation of masses [2,27] the frequency ratios r have to be converted into linear equations between the mass excess of the investigated and the reference nuclide. Equation (4) can be written in the form

$$ME - r \cdot ME_{\mathrm{ref}} = m_{\mathrm{e}}(1-r) + A_{\mathrm{ref}}\left(r - \frac{A}{A_{\mathrm{ref}}}\right), \quad (5)$$

with ME and ME_{ref} denoting the mass excesses and A and A_{ref} the mass numbers of the investigated and the reference nuclide, respectively (all masses are expressed in atomic mass units). If one defines C as a truncated three-digit approximation

$$C = \left(\frac{A}{A_{\mathrm{ref}}}\right)_{\mathrm{trunc}}, \quad (6)$$

one obtains the desired result

$$ME - C \cdot ME_{\mathrm{ref}} = MD\,, \quad (7)$$

with

$$MD = ME_{\mathrm{ref}}(r-C) + m_{\mathrm{e}}(1-r) + A_{\mathrm{ref}}\left(r - \frac{A}{A_{\mathrm{ref}}}\right). \quad (8)$$

Table 9 lists the data of the present work (see table 2) converted into linear relations. In addition the mass excess values for the nuclides investigated are presented. For calculating these, one has to use the mass excess values of the reference nuclides ^{85}Rb ($ME = -82167.687(2.332)$ keV) and ^{133}Cs ($ME = -88075.660(2.952)$ keV). However, the mass excess values are only listed for convenience and are not used as input data.

Appendix C.2. Resolution of conflicts

For some of the nuclides investigated there were discrepancies to mass values determined by other groups. These conflicts where resolved.

^{136}Pr and ^{136}Nd

There is a discrepancy between the value for the mass difference deduced from this work 2128(19) keV and the Q_β-value derived from a careful measurement of the K/β^+ ratio in the decay of ^{136}Nd to ^{136}Pr: $Q_\beta = 2211(25)$ keV by A.R. Brosi *et al.* [45].

However, a later work by W. Bambynek *et al.* [46] points out that there exists a systematic deviation between calculated and measured K/β^+ ratios, which seems to increase with proton number. From the Penning trap data presented in this work one can calculate a K/β^+ ratio of $K/\beta^+_{\mathrm{calc}} = 16.37$. Using the experimental ratio of $K/\beta^+_{\mathrm{exp}} = 13.2(9)$ [45], one obtains $(K/\beta^+_{\mathrm{exp}})/(K/\beta^+_{\mathrm{calc}}) \approx 0.8$ which is in agreement with the suggested trend [46].

The input value given by Brosi *et al.* [45] is therefore excluded from the evaluation and marked as "well-documented data which disagree with other well-documented values"[3].

$^{140\mathrm{m}}$Pm

The mass of the isomeric state $^{140\mathrm{m}}$Pm in the atomic mass evaluation of 1995 [27] is determined by a Q_β-value measurement by G.G. Kennedy *et al.* [47]. This value is in conflict, at a 3σ level, with the value obtained in the present work. The levels in ^{140}Nd fed by the decay of $^{140\mathrm{m}}$Pm were investigated. It is not clear from the publication whether the β-spectrum was recorded in coincidence with γ-rays emitted by the daughter nucleus. The activities of $^{140\mathrm{g}}$Pm and ^{141}Pm were taken into account by recording the β-spectra within different time intervals. However, the publication does not describe how other nuclides and isobars, that could also have been produced, were removed. The input value given in [47] is therefore excluded from the adjustment and marked as "well-documented data which disagree with other well-documented values".

^{141}Pm

The discrepancy with our value comes from a value given in the work by A. Charvet *et al.* [48]. In this work the nuclear levels of ^{141}Nd populated in the decay of ^{141}Pm were investigated. However, the description of the Q_β-measurement is very short. It is not mentioned if characteristic γ-lines have been used in coincidence with β-particles to determine the β-spectrum. In addition, the description of the β-spectrometer and its calibration is missing.

Thus, the datum from [48] is excluded from the least-squares adjustment and is marked by "well-documented data which disagree with other well-documented values".

^{139}Sm

In the atomic mass evaluation of 1993 the mass of ^{139}Sm was determined via Q_β-measurements by G.D. Alkhazov *et al.* [34] and J. Deslauriers *et al.* [49]. The yielded masses are 300–400 keV higher than the ISOLTRAP value. In [34] there is no description how the Q-values have been determined. In [49] the Z identification was achieved via characteristic X-rays and the β-spectrum was recorded in coincidence with the 306.7 keV γ-line, but no information is given on the calibration of the spectrometer.

In any case, the Q_β-values from [34,49] have much larger uncertainties (150 keV) than the ISOLTRAP value. Therefore they are excluded from the input data of the mass evaluation and marked by "data with much less weight than that of a combination of other data".

^{140}Sm

There exists a discrepancy of 468 keV between the ISOLTRAP value and that of J. Deslauriers *et al.* [50]. This value was not used in AME93 but replaced by a recommended value following from the regular trends of the atomic masses. Due to its large uncertainty of 300 keV

[3] The term "well-documented" means that this work is either published in a refereed journal or originates from another well-documented work.

Table 9. The data of the present work converted to linear relations. Column 1 lists the linear relations and column 2 gives the MD-values (see text). The mass excess values as obtained from the experimental result of the present work are given in column 3. Nuclides marked by u, v, w, x, y, z are special cases and discussed in the main text.

Linear relation	MD-value (μu)	Mass excess (keV)
^{133}Cs − 1.565 * ^{85}Rb	43500(13)	−88072(13)
^{123}Ba − 0.925 * ^{133}Cs	6238(13)	−75659(13)
^{125}Ba − 0.940 *^{133}Cs	3356(13)	−79665(12)
^{127}Ba − 0.955 * ^{133}Cs	1389(13)	−82818(12)
^{131}Ba − 0.985* ^{133}Cs	72(14)	−86687(13)
^{133}Pr − 1.000 *^{133}Cs	10877(15)	−77944(15)
^{134}Pr − 1.008 * ^{133}Cs	11029(16)	−78507(15)
^{135}Pr − 1.015 * ^{133}Cs	9080(14)	−80939(14)
^{136}Pr − 1.023 * ^{133}Cs	9418(15)	−81328(14)
^{137}Pr − 1.030 * ^{133}Cs	8095(15)	−83177(14)
^{130}Nd^{19}F^{v} − 1.120 * ^{133}Cs	32902(130)	−67997(121)
^{132}Nd − 0.992 * ^{133}Cs	17147(52)	−71399(48)
^{134}Nd − 1.008 * ^{133}Cs	14100(14)	−75646(13)
^{135}Nd^{z} − 1.015 * ^{133}Cs	14179(14)	−76189(14)
^{136}Nd − 1.023 * ^{133}Cs	11703(14)	−79200(13)
^{137}Nd − 1.030 * ^{133}Cs	11947(14)	−79589(13)
^{138}Nd − 1.038 * ^{133}Cs	10093(14)	−82021(14)
^{136m}Pm^{x} − 1.023 * ^{133}Cs	20429(20)	−71072(19)
^{137}Pm − 1.030 * ^{133}Cs	17864(14)	−74077(14)
^{138}Pm − 1.038 * ^{133}Cs	17721(14)	−74916(13)
^{139}Pm − 1.045 * ^{133}Cs	15604(15)	−77504(14)
^{140m}Pm − 1.053 * ^{133}Cs	16064(16)	−77780(15)
^{141}Pm − 1.060 * ^{133}Cs	13776(15)	−80528(14)
^{143}Pm − 1.075 * ^{133}Cs	12567(15)	−82975(14)
^{136}Sm − 1.023 * ^{133}Cs	25009(15)	−66806(14)
^{137}Sm^{y} − 1.030 * ^{133}Cs	24447(14)	−67946(13)
^{138}Sm − 1.038 * ^{133}Cs	21387(14)	−71500(13)
^{139}Sm − 1.045 * ^{133}Cs	21101(14)	−72383(13)
^{140}Sm − 1.053 * ^{133}Cs	18557(15)	−75458(14)
^{141g}Sm − 1.060 * ^{133}Cs	18694(14)	−75947(14)
^{141m}Sm − 1.060 * ^{133}Cs	18878(14)	−75776(14)
^{142}Sm − 1.068 * ^{133}Cs	16173(14)	−79000(14)
^{143}Sm − 1.075 * ^{133}Cs	16268(15)	−79528(14)
^{139}Eu − 1.045 * ^{133}Cs	28597(16)	−65401(15)
^{141}Eu − 1.060 * ^{133}Cs	25164(15)	−69920(14)
^{142m}Eu − 1.068 * ^{133}Cs	24909(15)	−70862(14)
^{143}Eu − 1.075 * ^{133}Cs	21947(14)	−74238(14)
^{144}Eu − 1.083* ^{133}Cs	21223(17)	−75617(16)
^{145}Eu − 1.090* ^{133}Cs	19338(17)	−77989(16)
^{146}Eu − 1.098* ^{133}Cs	21029(15)	−77119(15)
^{147}Eu − 1.105* ^{133}Cs	21215(16)	−77562(16)
^{148}Eu − 1.113* ^{133}Cs	23315(15)	−76310(15)
^{149}Eu -1.120* ^{133}Cs	23849(17)	−76429(16)
^{151}Eu − 1.776* ^{85}Rb	76520(15)	−74652(15)
^{153}Eu − 1.800* ^{85}Rb	80021(16)	−73363(15)
^{148}Dy − 1.113* ^{133}Cs	32394(16)	−67853(15)
^{149}Dy^{w} − 1.120* ^{133}Cs	33278(109)	−67647(101)
^{154}Dy^{v} − 1.158* ^{133}Cs	33903(19)	−70411(18)
^{150}Ho − 1.128* ^{133}Cs	40150(29)	−61950(27)

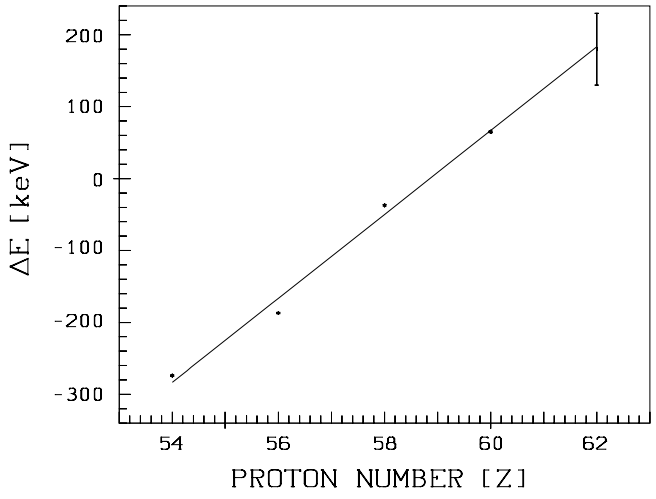

Fig. 11. Energy differences between the $I = 1/2^+$ and the $I = 9/2^-$ (or $I = 11/2^-$ in the case of ^{129}Xe) states of some even-odd nuclei along the $N = 75$ line [22]. The energy difference for ^{137m}Sm ($Z = 62$) has been extrapolated in [22] with a conservative error of 50 keV. The solid line is a fit of a linear function through the data points.

the Q_β-value of [50] is now not used and marked by "data with much less weight than that of a combination of other data".

^{148}Eu

Between the atomic mass evaluation of 1995 and the data presented in this work there exists a discrepancy of 71 keV. The value given in the mass evaluation is an average of three different works; two Q_β-measurements by C.V.K. Baba *et al.* [51] and V.A. Ageev *et al.* [52] and a Q_α-measurement by K.S. Toth *et al.* [53]. The Q_β-values agree remarkably well but they disagree with the result from the present work by 100 keV. On the other hand, the Q_α-measurement is in good agreement with the ISOLTRAP data.

The documentation of [51] is complete and gives an endpoint energy of 920(30) keV for the decay into the 1162 keV or the 1181 keV level.

The same decay channel has been examined in [52]. However, the origin and preparation of the radioactive source remain unclear: "... using an 'old' europium preparation containing ^{148}Eu and ^{149}Eu ...". It is also not clear whether the β-spectrum was recorded in coincidence with γ-lines of the daughter ^{148}Sm. Some doubt on this value arises also from the erroneous Q-value measurement following the decay of ^{146}Gd.

The input values by Baba *et al.* and Ageev *et al.* [51, 52] are therefore excluded from the input data and marked by "well-documented data which disagree with other well-documented values".

Appendix C.3. Special treatment for some ISOLTRAP data

^{130}Nd^{19}F

While the mass of ^{19}F is well known, there exists no experimental information on the ground-state mass of ^{130}Nd, it having been only estimated from systematic trends. In order to obtain a first experimental result on ^{130}Nd, the ISOLTRAP datum on ^{130}Nd^{19}F is combined with the ground-state mass of ^{19}F. However, the result on ^{130}Nd^{19}F is only tentative due to its very poor statistics.

^{135}Nd

As discussed in appendix B.1, a mixture of ground and isomeric states has been investigated by ISOLTRAP. The resulting frequency ratio is now combined with the known excitation energy of the isomer $\Delta E = 65.1$ keV and the mixing ratio of both states. From the spins and half-lives it is assumed that both states are delivered with the same amount by ISOLDE.

^{136}Pm

Since a contamination by another long-lived state of this nucleus cannot be excluded (see appendix B.2.2), the uncertainty of the value for ^{136x}Pm as determined in this work was increased from 20 μu to 100 μu. Initially it was not clear which of the states of this nucleus was investigated. The "Nuclear Data Sheets" of January 1994 indicate that G.D. Alkhazov *et al.* investigated the state with spin $I = 5^+$ of ^{136}Pm which has a half-life of $T_{1/2} = 107(6)$ s [34]. By comparing the mass values one finds that the state investigated by Alkhazov *et al.* is more strongly bound than the state investigated by ISOLTRAP. Therefore, the ISOLTRAP value has to be assigned to the isomeric state ($I = 2^+$, $T_{1/2} = 47(2)$).

^{137}Sm

Systematic trends indicate the existence of an isomer with spin $I = 1/2^+$. Figure 11 shows the energy differences of the $I = 9/2^-$ (or $I = 11/2^-$ in the case of ^{129}Xe) and $I = 1/2^+$ levels of some even-odd nuclei along the $N = 75$ line. By extrapolating the measured energy differences for these two levels from the range $54 \leq Z \leq 60$, the energy difference for ^{137}Sm can be estimated at $\Delta E = 180(50)$ keV. If one assumes that the ratio of the half-lives of the $I = 9/2^-$ and $I = 1/2^+$ states is similar to the one in ^{135}Nd ($N = 75$), one can estimate the half-life of the $I = 1/2^+$ state. Using the half-life of $T_{1/2} = 51(1)$ s for the ground state, one obtains $T_{1/2} \approx 20$ s for the isomer ^{137m}Sm.

If the isomeric state exists one expects that it is produced with a yield that is of the same order of magnitude as the yield of the ground state. Since the mass difference between the two species is smaller than the width of the resonance curve, the cyclotron frequency of their mean mass would be measured. However, to now there is no experimental proof for the existence of the isomer. The estimated excitation energy of the isomer can therefore not be used to correct the experimental result for ^{137}Sm.

The experimental result of this work on ^{137y}Sm is thus assigned to the ground state.

References

1. J. Blomqvist et al., Z. Phys. A **312**, 27 (1983).
2. G. Audi, A.H. Wapstra, Nucl. Phys. A **565**, 193 (1993).
3. For an overview see *Proceedings of Nobel Symposium 91 "Trapped Charged Particles and Related Fundamental Physics"* (Lysekil, Sweden, 1994), Phys. Scr. **T59** (1995).
4. B. Schlitt et al., Hyperfine Interact. **99**, 117 (1996).
5. M.P. Bradley et al., Phys. Rev. Lett. **83**, 4510 (1999).
6. C. Carlberg et al., Phys. Rev. Lett. **83**, 4506 (1999).
7. G. Bollen et al., Nucl. Instrum. Methods A **368**, 675 (1996).
8. E. Kugler et al., Nucl. Instrum. Methods B **70**, 41 (1992).
9. B. Jonson et al., Nucl. Phys. News **3**, 5 (1993).
10. G. Bollen et al., Phys. Rev. C **46**, R2140 (1992).
11. H. Stolzenberg et al., Phys. Rev. Lett. **65**, 3104 (1990).
12. G. Bollen et al., J. Mod. Opt. **39**, 257 (1992).
13. T. Otto, *Penningfallenmassenspektrometrie an neutronenarmen Rubidium-und Strontium-Isotopen*, Ph.D. thesis, Mainz, Germany (1993).
14. H. Raimbault-Hartmann et al., Nucl. Instrum. Methods B **126**, 378 (1997).
15. T. Radon et al., submitted to Nucl. Phys. A.
16. G. Bollen et al., *A Radio Frequency Quadrupole Ion Beam Buncher for ISOLTRAP*, in *Proceedings of the 2nd International Conference on Exotic Nuclei and Atomic Masses, Bellaire, Michigan, USA, June 23-27, 1998*, edited by B.M. Sherill, D.J. Morrisey, C.N. Davids, AIP Conf. Proc. **455**, 965 (1998).
17. G. Savard et al., Phys. Lett. A **158**, 247 (1991).
18. M. König et al., Int. J. Mass Spectrosc. Ion. Proc. **142**, 95 (1995).
19. D. Beck, *Massenbestimmung instabiler Isotope der Seltenen Erden um* ^{146}Gd *mit dem ISOLTRAP-Spektrometer*, Ph.D. thesis, Mainz, Germany (1997).
20. E. Schark, *Erste direkte Massenbestimmung radioaktiver Isotope Seltener Erden am ISOLTRAP-Experiment*, Ph.D. thesis, Mainz, Germany (1997).
21. D. Beck et al., Nucl. Phys. A **626**, 343 (1998).
22. G. Audi et al., Nucl. Phys. A **624**, 1 (1997).
23. G. Bollen et al., J. Appl. Phys. **68**, 4355 (1990).
24. L.S. Brown, G. Gabrielse, Rev. Mod. Phys. **58**, 233 (1986).
25. D. Beck et al., Nucl. Instrum. Methods B **126**, 374 (1997).
26. F. Ames et al., Nucl. Phys. A **651**, 3 (1999).
27. G. Audi, A.H. Wapstra, Nucl. Phys. A **595**, 409 (1995).
28. W.D. Myers, W.J. Swiatecki, Nucl. Phys. **81**, 1 (1966).
29. T. Kozlowski et al., *Program of the 27th USSR Conference on Nuclear Spectroscopy* (1977) p. 65.
30. J.M. D'Auria et al., Phys. Rev. **172**, 1176 (1968).
31. G. Beyer et al., Nucl. Phys. A **260**, 269 (1976).
32. T.H. Handley et al., Phys. Rev. **96**, 1003 (1954).
33. G.G. Kennedy et al., Phys. Rev. C **12**, 553 (1975).
34. G.D. Alkhazov et al., Z. Phys. A **310**, 247 (1983).
35. A.V. Potempa et al., Izv. Akad. Nauk SSSR **58**, 41 (1994).
36. G.D. Alkhazov et al., Z. Phys. A **344**, 425 (1993).
37. R.C. Barber et al., Phys. Rev. Lett. **12**, 597 (1964).
38. C.N. Davids et al., Phys. Rev. C **55**, 2255 (1997).
39. G.D. Alkhazov et al., Z. Phys. A **311**, 245 (1983).
40. S. Liran, N. Zeldes, At. Data Nucl. Data Tables **17**, 431 (1976).
41. J. Szerypo, private communication (1997).
42. G. Audi, *Mesures de Mass Atomiques de Noyaux Exotiques*, Ph.D thesis., Orsay, France (1981).
43. H. Ravn, private communication (1996).
44. T. Bjørnstad et al., Phys. Scr. **34**, 578 (1986).
45. A.R. Brosi et al., Nucl. Phys. A **245**, 243 (1975).
46. W. Bamynek et al., Rev. Mod. Phys. **49**, 1 (1977).
47. G.G. Kennedy et al., Z. Phys. A **274**, 233 (1975).
48. A. Charvet et al., J. Phys., **31**, 737 (1970).
49. J. Deslauriers et al., Phys. Rev. C **25**, 504 (1982).
50. J. Deslauriers et al., Z. Phys. A **326**, 155 (1987).
51. C.V.K. Baba et al., Nucl. Phys. **43**, 285 (1963).
52. V.A. Ageev et al., Izv. Akad. Nauk SSSR **34**, 345 (1970).
53. K.S. Toth et al., Phys. Rev. B **136**, 1233 (1964).